Non-equilibrium quantum theory for nanodevices based on the Feynman–Vernon influence functional

2010 New J. Phys. 12 083013

(http://iopscience.iop.org/1367-2630/12/8/083013)

New Journal of Physics
The open-access journal for physics

Non-equilibrium quantum theory for nanodevices based on the Feynman–Vernon influence functional

Jinshuang Jin[1,2], Matisse Wei-Yuan Tu[1], Wei-Min Zhang[1,4] and YiJing Yan[3]

[1] Department of Physics and Center for Quantum Information Science, National Cheng Kung University, Tainan 70101, Taiwan
[2] Department of Physics, Hangzhou Normal University, Hangzhou 310036, People's Republic of China
[3] Department of Chemistry, Hong Kong University of Science and Technology, Kowloon, Hong Kong
E-mail: wzhang@mail.ncku.edu.tw

New Journal of Physics **12** (2010) 083013 (30pp)
Received 20 May 2010
Published 6 August 2010
Online at http://www.njp.org/
doi:10.1088/1367-2630/12/8/083013

Abstract. In this paper, we present a non-equilibrium quantum theory for transient electron dynamics in nanodevices based on the Feynman–Vernon influence functional. Applying the exact master equation for nanodevices we recently developed to the more general case in which all the constituents of a device vary in time in response to time-dependent external voltages, we obtained non-perturbatively the transient quantum transport theory in terms of the reduced density matrix. The theory enables us to study transient quantum transport in nanostructures with back-reaction effects from the contacts, with non-Markovian dissipation and decoherence being fully taken into account. For a simple illustration, we apply the theory to a single-electron transistor subjected to ac bias voltages. The non-Markovian memory structure and the nonlinear response functions describing transient electron transport are obtained.

[4] Author to whom any correspondence should be addressed.

Contents

1. Introduction

The investigation of quantum coherence dynamics far away from equilibrium in nanoscale quantum devices (nanodevices) has attracted much attention in the past decade, due to various applications in nanotechnology and quantum information processing. Experimentally, it became possible not only to directly manufacture structures but also to investigate their non-equilibrium quantum coherence properties under well-controlled parameters [1]–[5]. Previous theoretical investigations focused mainly on the steady-state limit of the non-equilibrium quantum transport [6]–[8]. More recently, increasing efforts have been devoted to the study of the time-dependent quantum transport far away from equilibrium [9]–[15]. In fact, *a full understanding of non-equilibrium dynamics induced and controlled by external fields lies in the temporal evolution of electrons in nanodevices from some specific initial preparation towards any designed state within an extremely short time,* which is essential for practical applications.

Prototypical nanodevices studied in this paper are made of a gate-defined region on a semiconductor containing discrete electronic states or a quasi-continuum spectrum, as shown in figure 1. Electrode leads are implanted around this central region to control the electrons across it. Also, gates are deposited to adjust the electronic states within the central area as well as their couplings to the surrounding electrodes. Much theoretical work has been devoted to the understanding and prediction of how fast or slow the device can turn a current on or off. However, as a quantum device, in particular for quantum information processing [2]–[5], the big challenge is to understand and predict not only how fast or slow the device can turn a current on or off but also how reliably and efficiently the device can manipulate quantum coherence of the

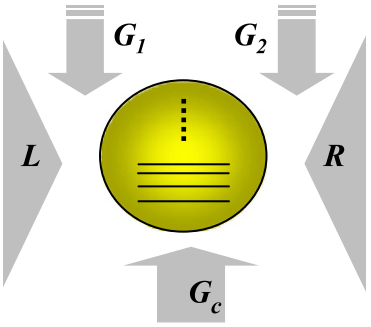

Figure 1. A schematic plot of a nanoscale quantum device in which the bias voltage is applied to the source, and the drain electrode leads labeled L and R and other gates labeled $G_c, G_1, G_2, \ldots$ control the energy levels of the central region as well as the couplings between the central region and the leads.

electron states through external bias and gate voltage controls. This requires a non-equilibrium quantum device theory to fully analyze the quantum coherence dynamics of electrons in the device. The purpose of this paper is to attempt to establish such a nonequilibrium theory for the quantum coherence dynamics of electrons in nanodevices that can be feedback controlled through the nonlinear response of the electron transport to the external time-dependent bias and gate voltage pulses.

Physically, the nanodevice studied in this paper is a typical open quantum system in the sense that it exchanges particles, energy and information with its surroundings. *For an open quantum system, the non-equilibrium electron dynamics are completely determined by the master equation of the reduced density matrix* $\rho(t)$, *which can fully depict the dynamics of electron quantum coherence in the device.* Any other physical observable is simply given by $\langle O(t)\rangle = \langle O\rho(t)\rangle$. The transient electron transport should also be directly solved from the reduced density matrix. However, it has been attempted for many years without a very satisfactory answer to find the exact master equation for an arbitrary open quantum system [16]. Most of the master equations used in the literature are obtained using semiclassical approximation or perturbation truncation, such as the semiclassical Boltzmann equation [17, 18] or the Lindblad-type master equations under the Born–Markov approximation [19]. For a nanodevice with an extremely short length scale ($\sim$1 nm) and extremely fast time scale ($\sim$1 fs), the semiclassical Boltzmann equation and the master equation under the Born–Markov approximation are most likely inapplicable.

Theoretically, there are two fundamental but equivalent methods for dealing with modern non-equilibrium physics. These are the Schwinger–Keldysh non-equilibrium Green function technique [20, 21] and the Feynman–Vernon influence functional approach [22]. In practical applications, both methods have their own advantages and disadvantages. The Schwinger–Keldysh non-equilibrium Green function technique allows not only a systematic perturbative study [23, 24] but also a non-perturbative study [25, 26] for various nonequilibrium phenomena in many-body systems. In particular, it is a powerful tool to study the steady-state properties, for which the initial state of the quantum system is irrelevant and where transport is mainly determined by the density of states [7, 8]. The extension of this method to treat time-dependent transport has already been investigated [27]. However, except for

the wide band limit (WBL), the time-dependent non-equilibrium Green function calculations become rather complicated, due to the initial state dependence and the non-Markovian memory structure [9, 12].

On the other hand, the Feynman–Vernon influence functional approach [22] is mainly used to study dissipation dynamics in quantum tunneling problems [28] and decoherence problems in quantum measurement theory [29]. It is, in particular, very useful to derive non-perturbatively the master equation for the reduced density matrix of an open system. This is accomplished by integrating out completely the environmental degrees of freedom through the path integral approach, where the non-Markovian memory structure is manifested explicitly. In the early applications of the influence functional approach, the master equation was derived for some particular class of Ohmic (white-noise) environments for the quantum Brownian motion (QBM), modeled as a central harmonic oscillator linearly coupled to a set of harmonic oscillators simulating the thermal bath [30, 31]. The exact master equation for the QBM with a general spectral density (color-noise environments) that can fully address the non-Markovian dynamics was the Hu–Paz–Zhang master equation [32]. Applications of the QBM exact master equation cover various topics, such as quantum decoherence, quantum-to-classical transition, quantum measurement theory, quantum gravity and quantum cosmology [19, 33, 34]. However, using the influence functional approach to obtain the exact master equation has largely been focused on the bosonic (thermal) environments in the past half century.

Meanwhile, utilizing the master equation to study quantum electron transport has also recently received a certain amount of attention. In principle, the master equation can be formally expressed in terms of the real-time diagrammatic expansion up to all the orders [35]–[37]. In practice, most of the master equation approaches used in quantum transport by far only take the perturbative theory up to the second order [38]–[40]. An exception is the recently developed hierarchical expansion [10]. This hierarchical expansion is a very efficient tool for the numerical study of the quantum transport properties, including the accurate evaluations of the Coulomb blockage and the Kondo transition dynamics [15, 41]. Still, a close form of the master equation for the reduced density matrix combined with the fully non-equilibrium electron transport dynamics in nanodevices has not yet been presented.

By extending the influence functional approach to the fermionic reservoirs, we have recently derived an exact master equation for a large class of nanodevices [13]. This exact master equation is capable of studying the full non-Markovian decoherence dynamics of electrons in nanostructures. In the present work, we shall extend the exact master equation to the cases in which all the constituents of a device, including the couplings to leads, vary in time in response to time-dependent external voltages. We then derive the exact quantum transport theory in terms of the reduced density matrix within the same framework. The resulting theory can be used to investigate various time-dependent quantum transport processes accompanied explicitly by non-Markovian quantum relaxation and decoherence dynamics. The non-equilibrium transport based on Keldysh's Green function technique can be easily reproduced from the present theory.

The remainder of this paper is organized as follows. In section 2, we outline the derivation of the exact master equation we obtained recently [13], with the extension to the time-dependent Hamiltonian. In section 3, we derive the transient current operator in terms of the reduced density operator, based on the influence functional and the master equation. The relation between the reduced density matrix and the time-dependent current is established through the master equation, and all the back-reaction effects associated with the non-Markovian dynamics of electrons are fully taken into account. As an illustration, we apply the theory to a

single-electron transistor (SET) subjected to ac bias voltages in section 4, where the non-Markovian memory structure and the nonlinear response functions describing transient electron transport are obtained. The summary and perspective are given in section 5. In the appendices, a close connection between the exact master equation approach and the non-equilibrium Green function technique for transient quantum transport is established.

2. The exact master equation of the reduced density matrix for nanodevices

In this section, we shall outline the exact master equation derived recently by two of us for a large class of nanodevices [13], with an extension to the time-dependent energy levels and couplings. We shall only list the necessary formulae that we will use later for the derivation of the transient current. For a more detailed derivation, please refer to [13]. We begin with the Hamiltonian of a prototypical mesoscopic system for electron transport,

$$H(t) = \sum_{ij} \epsilon_{ij}(t) a_i^\dagger a_j + \sum_{\alpha k} \epsilon_{\alpha k}(t) c_{\alpha k}^\dagger c_{\alpha k} + \sum_{i\alpha k} [V_{i\alpha k}(t) a_i^\dagger c_{\alpha k} + V_{i\alpha k}^*(t) c_{\alpha k}^\dagger a_i]. \quad (1)$$

Here, the first sum represents the electron Hamiltonian H_S for the central region in the device. The second sum represents the Hamiltonian $\sum_\alpha H_\alpha$ describing the non-interacting electron leads (the source and drain electrodes, plus other electric gates; see figure 1) labeled by the index $\alpha(=L, R, \ldots)$. The last term is the electron tunneling Hamiltonian H_T between the leads and the central region. To make the transient dynamics complete, the bias voltages V_α applied to the leads are considered to be a time-dependent external field or an ultrafast pulse such that the single-electron energy levels in the leads are shifted as $\epsilon_{\alpha k} \to \epsilon_{\alpha k}(t) = \epsilon_{\alpha k} + eV_\alpha(t)$. In principle, a time-dependent external field may also induce off-diagonal terms to the electrode Hamiltonian in the single-electron energy basis, but it is not difficult to transform it into a new diagonal basis as long as the external field does not induce electron–electron interactions in the electrode leads. Meanwhile, the energy levels ϵ_{ij} of the central region and the couplings $V_{i\alpha k}$ between the central region and the leads are controllable through the gate voltages and external field pulses so that they can be, in general, also time dependent: $\epsilon_{ij} \to \epsilon_{ij}(t) = \epsilon_{ij} + \Delta_{ij}(t)$ and $V_{i\alpha k} \to V_{i\alpha k}(t)$. Throughout this work, we set $\hbar = 1$, except for the transient current where we will put $\hbar$ back into its definition.

It is worth noting that we have not considered the electron–electron Coulomb interaction in equation (1), which may induce interesting new phenomena, such as the Kondo effect at very low temperature [42]. However, in practical applications, the importance of Coulomb correlations depends on the energy scale involved in the manipulation of nanodevices. One can always control the energy scale of the nanodevice to let the Coulomb correlations become negligible or to set up the device in the Coulomb blockage regime for practical applications. For the Coulomb blockage regime, as we have shown, we can properly and explicitly exclude the doubly occupied states and the resulting master equation can be applied to the strong Coulomb repulsion [13]. Therefore, these two extreme limits, the extremely weak and the extremely strong Coulomb interaction regimes together, can cover most of the useful nanodevices. The extension to the general Coulomb interaction regime will then be retained for further investigation.

Our derivation of the master equation is based on the Feynman–Vernon influence functional approach [22, 28, 32] in the coherent state representation [13]. As is well known [16], the

non-equilibrium electron dynamics of an open system are completely determined by the so-called reduced density matrix. The reduced density matrix is defined from the density matrix of the total system (the central system plus the leads, and the leads are treated as reservoirs to the central system) by tracing over entirely the environmental degrees of freedom: $\rho(t) \equiv \mathrm{tr}_{\mathrm{R}}[\rho_{\mathrm{tot}}(t)]$, where the total density matrix is formally given by $\rho_{\mathrm{tot}}(t) = U(t, t_0)\rho_{\mathrm{tot}}(t_0)U^{\dagger}(t, t_0)$ with the evolution operator $U(t, t_0) = T\exp\{-\mathrm{i}\int_{t_0}^{t} H(\tau)\mathrm{d}\tau\}$, and T is the time-ordering operator. As usual, we assume that the central region is uncorrelated with the reservoirs before the tunneling couplings are turned on [28]: $\rho_{\mathrm{tot}}(t_0) = \rho(t_0) \otimes \rho_R(t_0)$, where the system can be in an arbitrary state $\rho(t_0)$ but the reservoirs are initially at equilibrium: $\rho_{\mathrm{R}}(t_0) = \frac{1}{Z}\mathrm{e}^{-\sum_{\alpha}\beta_{\alpha}(H_{\alpha}-\mu_{\alpha}N_{\alpha})}$, $\beta_{\alpha} = 1/(k_{\mathrm{B}}T_{\alpha})$ is the initial inverse temperature and $N_{\alpha} = \sum_k c_{\alpha k}^{\dagger}c_{\alpha k}$ is the particle number operator for the lead α.

In the coherent state representation [13, 43, 44], the reduced density matrix at an arbitrary later time t can be expressed as

$$\langle \boldsymbol{\xi}_f|\rho(t)|\boldsymbol{\xi}_f'\rangle = \int \mathrm{d}\mu(\boldsymbol{\xi}_0)\,\mathrm{d}\mu(\boldsymbol{\xi}_0')\langle \boldsymbol{\xi}_0|\rho(t_0)|\boldsymbol{\xi}_0'\rangle \mathcal{J}(\bar{\boldsymbol{\xi}}_f, \boldsymbol{\xi}_f', t|\boldsymbol{\xi}_0, \bar{\boldsymbol{\xi}}_0', t_0), \tag{2}$$

with $\boldsymbol{\xi} = (\xi_1, \xi_2, \ldots)$ and $\bar{\boldsymbol{\xi}} = (\xi_1^*, \xi_2^*, \ldots)$ being the Grassmannian numbers and their complex conjugate defined through the fermion coherent states: $a_i|\boldsymbol{\xi}\rangle = \xi_i|\boldsymbol{\xi}\rangle$ and $\langle\boldsymbol{\xi}|a_i^{\dagger} = \langle\boldsymbol{\xi}|\xi_i^*$. The propagating function in equation (2) is given in terms of Grassmannian number path integrals,

$$\mathcal{J}(\bar{\boldsymbol{\xi}}_f, \boldsymbol{\xi}_f', t|\boldsymbol{\xi}_0, \bar{\boldsymbol{\xi}}_0', t_0) = \int \mathcal{D}[\bar{\boldsymbol{\xi}}\boldsymbol{\xi}; \bar{\boldsymbol{\xi}}'\boldsymbol{\xi}']\mathrm{e}^{\mathrm{i}(S_{\mathrm{c}}[\bar{\boldsymbol{\xi}},\boldsymbol{\xi}]-S_{\mathrm{c}}^{*}[\bar{\boldsymbol{\xi}}',\boldsymbol{\xi}'])}\mathcal{F}[\bar{\boldsymbol{\xi}}\boldsymbol{\xi}; \bar{\boldsymbol{\xi}}'\boldsymbol{\xi}'], \tag{3}$$

where $S_{\mathrm{c}}[\bar{\boldsymbol{\xi}}, \boldsymbol{\xi}]$ is the action of the central system in the fermion coherent state representation and $\mathcal{F}[\bar{\boldsymbol{\xi}}\boldsymbol{\xi}; \bar{\boldsymbol{\xi}}'\boldsymbol{\xi}']$ is the influence functional obtained after integrating out all the environmental (reservoirs) degrees of freedom [13]:

$$\begin{aligned}\mathcal{F}[\bar{\boldsymbol{\xi}}\boldsymbol{\xi}; \bar{\boldsymbol{\xi}}'\boldsymbol{\xi}'] = \exp\Bigg\{ &-\sum_{\alpha ij}\int_{t_0}^{t}\mathrm{d}\tau\int_{t_0}^{\tau}\mathrm{d}\tau'(\boldsymbol{g}_{\alpha ij}(\tau,\tau')\xi_i^*(\tau)\xi_j(\tau') + \boldsymbol{g}_{\alpha ji}^*(\tau,\tau')\xi_i'^*(\tau')\xi_j'(\tau)) \\ &-\sum_{\alpha ij}\int_{t_0}^{t}\mathrm{d}\tau\int_{t_0}^{t}\mathrm{d}\tau'(\boldsymbol{g}_{\alpha ij}(\tau,\tau')\xi_i'^*(\tau)\xi_j(\tau') - \widetilde{\boldsymbol{g}}_{\alpha ij}(\tau,\tau') \\ &\times(\xi_i^*(\tau)+\xi_i'^*(\tau))(\xi_j(\tau')+\xi_j'(\tau'))\Bigg\}.\end{aligned} \tag{4}$$

The non-local time correlations in equation (4) are defined by

$$\boldsymbol{g}_{\alpha ij}(\tau,\tau') = \sum_k V_{i\alpha k}(\tau)V_{j\alpha k}^*(\tau')\mathrm{e}^{-\mathrm{i}\int_{\tau'}^{\tau}\mathrm{d}\tau_1\epsilon_{\alpha k}(\tau_1)}, \tag{5a}$$

$$\widetilde{\boldsymbol{g}}_{\alpha ij}(\tau,\tau') = \sum_k V_{i\alpha k}(\tau)V_{j\alpha k}^*(\tau')f_{\alpha}(\epsilon_{\alpha k})\mathrm{e}^{-\mathrm{i}\int_{\tau'}^{\tau}\mathrm{d}\tau_1\epsilon_{\alpha k}(\tau_1)}, \tag{5b}$$

which depict all the time correlations of electrons in the leads through the couplings with the central region and $f_{\alpha}(\epsilon_{\alpha k}) = 1/(\mathrm{e}^{\beta_{\alpha}(\epsilon_{\alpha k}-\mu_{\alpha})}+1)$ is the Fermi distribution function of the lead α at the initial time t_0.

This influence functional takes fully into account the back-reaction effects of the reservoirs on the central system. It modifies the original action of the system into an effective one, $e^{(i/\hbar)(S_c[\bar{\xi},\xi]-S_c^*[\bar{\xi}',\xi'])}\mathcal{F}[\bar{\xi}\xi;\bar{\xi}'\xi'] = e^{(i/\hbar)S_{\rm eff}[\bar{\xi}\xi;\bar{\xi}'\xi']}$, which dramatically changes the dynamics of the central system. The detailed change is manifested through the generating function of equation (3) by carrying out the path integral with respect to the effective action $S_{\rm eff}[\bar{\xi}\xi;\bar{\xi}'\xi']$. The path integral $\mathcal{D}[\bar{\xi}\xi;\bar{\xi}'\xi']$ integrates over all the forward paths $\bar{\xi}(\tau)$, $\xi(\tau)$ and the backward paths $\bar{\xi}'(\tau)$, $\xi'(\tau)$ in the Grassmannian space bounded by $\bar{\xi}(t)=\bar{\xi}_f$, $\xi(t_0)=\xi_0$ and $\bar{\xi}'(t_0)=\bar{\xi}'_0$, $\xi'(t)=\xi'_f$, respectively. Since $S_{\rm eff}[\bar{\xi}\xi;\bar{\xi}'\xi']$ is only a quadratic function in terms of the integral variables, the path integrals in equation (3) can be reduced to Gaussian integrals so that we can use the stationary path method to exactly carry them out [45][5]. The resulting generating function is [13]

$$\mathcal{J}(\bar{\xi}_f,\xi'_f,t|\xi_0,\bar{\xi}'_0,t_0)=\frac{1}{\det[\boldsymbol{w}(t)]}\exp\{\bar{\xi}_f\boldsymbol{J}_1(t)\xi_0+\bar{\xi}_f\boldsymbol{J}_2(t)\xi'_f+\bar{\xi}'_0\boldsymbol{J}_3(t)\xi_0+\bar{\xi}'_0\boldsymbol{J}_1^{\dagger}(t)\xi'_f\},\tag{6}$$

in which the time-dependent coefficients are given explicitly as $\boldsymbol{J}_1(t)=\boldsymbol{w}(t)\boldsymbol{u}(t)$, $\boldsymbol{J}_2(t)=\boldsymbol{w}(t)-\boldsymbol{I}$ and $\boldsymbol{J}_3(t)=\boldsymbol{u}^{\dagger}(t)\boldsymbol{w}(t)\boldsymbol{u}(t)-\boldsymbol{I}$, with $\boldsymbol{w}(t)=[I-\boldsymbol{v}(t)]^{-1}$. Here, we have also expressed the stationary paths in terms of $N\times N$ matrix functions $\boldsymbol{u}(\tau)$, $\boldsymbol{v}(\tau)$ and $\bar{\boldsymbol{u}}(\tau)$ for $t_0\leqslant\tau\leqslant t$, where N is the total number of single-particle energy levels in the central region. They satisfy the following integrodifferential equations of motion (i.e. the stationary path equations of motion),

$$\dot{\boldsymbol{u}}(\tau)+i\boldsymbol{\epsilon}(\tau)\boldsymbol{u}(\tau)+\sum_{\alpha}\int_{t_0}^{\tau}d\tau'\boldsymbol{g}_{\alpha}(\tau,\tau')\boldsymbol{u}(\tau')=0,\tag{7a}$$

$$\dot{\bar{\boldsymbol{u}}}(\tau)+i\boldsymbol{\epsilon}(\tau)\bar{\boldsymbol{u}}(\tau)-\sum_{\alpha}\int_{\tau}^{t}d\tau'\boldsymbol{g}_{\alpha}(\tau,\tau')\bar{\boldsymbol{u}}(\tau')=0,\tag{7b}$$

$$\dot{\boldsymbol{v}}(\tau)+i\boldsymbol{\epsilon}(\tau)\boldsymbol{v}(\tau)+\sum_{\alpha}\int_{t_0}^{\tau}d\tau'\boldsymbol{g}_{\alpha}(\tau,\tau')\boldsymbol{v}(\tau')=\sum_{\alpha}\int_{t_0}^{t}d\tau'\tilde{\boldsymbol{g}}_{\alpha}(\tau,\tau')\bar{\boldsymbol{u}}(\tau'),\tag{7c}$$

subject to the boundary conditions $\boldsymbol{u}(t_0)=\boldsymbol{1}$, $\bar{\boldsymbol{u}}(t)=\boldsymbol{1}$ and $\boldsymbol{v}(t_0)=0$, where $\boldsymbol{g}_{\alpha}(\tau,\tau')$ and $\tilde{\boldsymbol{g}}_{\alpha}(\tau,\tau')$ are the non-local time correlation matrix functions, whose matrix elements are given by equation (5). As we show in appendix A, the matrix functions $\boldsymbol{u}(\tau)$, $\bar{\boldsymbol{u}}(\tau)$ and $\boldsymbol{v}(\tau)$ correspond, respectively, to the retarded, advanced and lesser Green functions, and $\boldsymbol{g}_{\alpha}(\tau,\tau')$ and $\tilde{\boldsymbol{g}}_{\alpha}(\tau,\tau')$ are the retarded and lesser self-energies in the non-equilibrium Green function technique. For the most general cases where all the parameters in Hamiltonian (1) are time dependent, the time translational invariance is broken. Then $\boldsymbol{u}(\tau)$ and $\bar{\boldsymbol{u}}(\tau)$ are independent except for the endpoints, where we have $\bar{\boldsymbol{u}}(t_0)=\boldsymbol{u}^{\dagger}(t)$. When all parameters in the Hamiltonian of equation (1) are time independent, $\boldsymbol{u}(\tau)$ becomes only a function of $\tau-t_0$ and $\bar{\boldsymbol{u}}(\tau)=\boldsymbol{u}^{\dagger}(t-\tau+t_0)$, as we have shown in [13].

Taking the time derivative of the reduced density matrix with the solution of the propagating function (6), together with the D-algebra of the fermion creation and annihilation

[5] Usually the stationary path (or stationary phase) method is an approximation to path integral calculations. When the path integrals can be reduced to Gaussian integrals, the stationary path method will lead to an exact solution. For a more detailed discussion, see [45].

operators in the fermion coherent state representation, we arrive at the final form of the exact master equation we obtained previously [13],

$$\frac{\mathrm{d}\rho(t)}{\mathrm{d}t} = -\mathrm{i}[H'_{\mathrm{S}}(t), \rho(t)] + \sum_{ij}\{\boldsymbol{\gamma}_{ij}(t)(2a_j\rho(t)a_i^\dagger - a_i^\dagger a_j\rho(t) - \rho(t)a_i^\dagger a_j) + \widetilde{\boldsymbol{\gamma}}_{ij}(t)(a_j\rho(t)a_i^\dagger - a_i^\dagger\rho(t)a_j - a_i^\dagger a_j\rho(t) + \rho(t)a_j a_i^\dagger)\}. \tag{8}$$

The first term (the commutator) in the master equation accounts for the renormalized effect (including the time-dependent shifts of the energy levels and the changes of the transition amplitudes between them) of the central system due to the coupling with the leads. The resulting renormalized Hamiltonian is $H'_{\mathrm{S}}(t) = \sum_{ij}\boldsymbol{\epsilon}'_{ij}(t)a_i^\dagger a_j$. The remaining terms in the master equation describe the dissipation and noise effects (which result in a non-unitary evolution of electrons in the central region) induced also by the coupling with the leads. All the time-dependent coefficients in equation (8) are determined systematically and explicitly by $\boldsymbol{u}(t)$ and $\boldsymbol{v}(t)$, as follows,

$$\begin{aligned}\boldsymbol{\epsilon}'_{ij}(t) &= \frac{\mathrm{i}}{2}[\dot{\boldsymbol{u}}\boldsymbol{u}^{-1} - (\boldsymbol{u}^\dagger)^{-1}\dot{\boldsymbol{u}}^\dagger]_{ij} \\ &= \boldsymbol{\epsilon}_{ij}(t) - \frac{\mathrm{i}}{2}\sum_\alpha[\boldsymbol{\kappa}_\alpha(t) - \boldsymbol{\kappa}_\alpha^\dagger(t)]_{ij},\end{aligned} \tag{9a}$$

$$\begin{aligned}\boldsymbol{\gamma}_{ij}(t) &= -\frac{1}{2}[\dot{\boldsymbol{u}}\boldsymbol{u}^{-1} + (\boldsymbol{u}^\dagger)^{-1}\dot{\boldsymbol{u}}^\dagger]_{ij} \\ &= \frac{1}{2}\sum_\alpha[\boldsymbol{\kappa}_\alpha(t) + \boldsymbol{\kappa}_\alpha^\dagger(t)]_{ij},\end{aligned} \tag{9b}$$

$$\begin{aligned}\widetilde{\boldsymbol{\gamma}}_{ij}(t) &= [\dot{\boldsymbol{u}}\boldsymbol{u}^{-1}\boldsymbol{v} + \boldsymbol{v}(\boldsymbol{u}^\dagger)^{-1}\dot{\boldsymbol{u}}^\dagger - \dot{\boldsymbol{v}}]_{ij} \\ &= \sum_\alpha[\boldsymbol{\lambda}_\alpha(t) + \boldsymbol{\lambda}_\alpha^\dagger(t)]_{ij}.\end{aligned} \tag{9c}$$

Here, we have used the relations solved from equation (7),

$$\boldsymbol{\kappa}_\alpha(t) = \int_{t_0}^t \mathrm{d}\tau\, \boldsymbol{g}_\alpha(t,\tau)\boldsymbol{u}(\tau)[\boldsymbol{u}(t)]^{-1}, \tag{10a}$$

$$\boldsymbol{\lambda}_\alpha(t) = \int_{t_0}^t \mathrm{d}\tau\{\boldsymbol{g}_\alpha(t,\tau)\boldsymbol{v}(\tau) - \widetilde{\boldsymbol{g}}_\alpha(t,\tau)\bar{\boldsymbol{u}}(\tau)\} - \boldsymbol{\kappa}_\alpha(t)\boldsymbol{v}(t). \tag{10b}$$

The master equation (8) takes a convolutionless form, so the non-Markovian dynamics are fully encoded in the time-dependent coefficients. These coefficients determined by the functions $\boldsymbol{u}(\tau)$, $\bar{\boldsymbol{u}}(\tau)$ and $\boldsymbol{v}(\tau)$ are governed essentially by integrodifferential equations (7). The non-local time correlation functions in equation (7), $\boldsymbol{g}_\alpha(\tau,\tau')$ and $\widetilde{\boldsymbol{g}}_\alpha(\tau,\tau')$, characterize all the non-Markovian memory structures of the central system interacting with its environment through the coupling Hamiltonian H_T. By solving equation (7), one can completely describe the quantum decoherence dynamics of electrons in the central region due to the entanglement between the central system and the leads. Master equation (8) is valid for various nanodevices coupled to

various surroundings as long as the electron–electron interaction can be ignored. It is also worth mentioning that the master equation is derived exactly so that the positivity, Hermiticity and trace of the reduced density matrix are guaranteed.

In fact, master equation (8) fully determines the exact non-equilibrium dynamics of open electron systems in nanostructures. The time dependence of an arbitrary physical observable is simply given by $\langle O(t)\rangle = \langle O\rho(t)\rangle$, which can be calculated from the master equation in a much simpler way since all the environmental degrees of freedom have already been eliminated completely. The transient electron transport can also be solved directly from the reduced density matrix. In the next section, we will first derive the transient current, in section 3.1, following the same approach of the influence functional. Then, in section 3.2, we will present an alternative derivation of the transient current based directly on master equation (8). As one can see, this derivation is rather simple in comparison with that in terms of the influence functional in section 3.1. Furthermore, in section 3.3, we will show the powerfulness of the master equation through a simpler but non-trivial calculation of the single-particle density matrix for arbitrary initial states of nanodevices.

3. Exact transient current for quantum transport

3.1. The influence functional approach

The transient current from the α-lead tunneling through the α-junction into the central region is defined in the Heisenberg picture as

$$I_\alpha(t) = -e\left\langle \frac{\mathrm{d}}{\mathrm{d}t}\hat{N}_\alpha(t)\right\rangle = \mathrm{i}\frac{e}{\hbar}\langle[\hat{N}_\alpha(t), H(t)]\rangle. \tag{11}$$

Here, e is the electron charge, $\langle O(t)\rangle \equiv \mathrm{tr}[O(t)\rho^H_{\mathrm{tot}}]$ with $\mathrm{tr}\equiv \mathrm{tr_S tr_R}$, $\hat{N}_\alpha(t) = \sum_k c^\dagger_{\alpha k}(t)c_{\alpha k}(t)$ and ρ^H_{tot} is the total density matrix in the Heisenberg picture. By explicitly calculating the above commutation relation with the Hamiltonian of equation (1) and then transforming it into the Schrödinger picture, we have

$$I_\alpha(t) = \mathrm{i}\frac{e}{\hbar}\,\mathrm{tr_S}\sum_i\left[A^\dagger_{\alpha i}(t)a_i - a^\dagger_i A_{\alpha i}(t)\right], \tag{12}$$

where the operators $A_{\alpha i}(t) = \mathrm{tr_R}[\sum_k V_{i\alpha k}(t)c_{\alpha k}\rho_{\mathrm{tot}}(t)]$ and $A^\dagger_{\alpha i}(t) = [A_{\alpha i}(t)]^\dagger$. The time dependence of these two operators comes from the non-Markovian memory dynamics by tracing the total density matrix over the environmental degrees of freedom in the Schrödinger picture. These two operators are indeed the effective (dressed) electronic creation and annihilation operators acting on the reduced density matrix of the central system, as a result of tracing over the reservoir degrees of freedom for the corresponding operators acting on the lead α.

Following the procedure of obtaining the reduced density matrix through the influence functional approach [13], we can write

$$\langle\boldsymbol{\xi}_f|A_{\alpha i}(t)|\boldsymbol{\xi}'_f\rangle = \int \mathrm{d}\mu(\boldsymbol{\xi}_0)\mathrm{d}\mu(\boldsymbol{\xi}'_0)\langle\boldsymbol{\xi}_0|\rho(t_0)|\boldsymbol{\xi}'_0\rangle\mathcal{J}^A_{\alpha i}(\bar{\boldsymbol{\xi}}_f, \boldsymbol{\xi}'_f, t|\boldsymbol{\xi}_0, \bar{\boldsymbol{\xi}}'_0, t_0), \tag{13}$$

where the operator-associated propagating function is defined as

$$\mathcal{J}^A_{\alpha i}(\bar{\boldsymbol{\xi}}_f, \boldsymbol{\xi}'_f, t|\boldsymbol{\xi}_0, \bar{\boldsymbol{\xi}}'_0, t_0) = \int \mathcal{D}[\bar{\boldsymbol{\xi}}\boldsymbol{\xi}; \bar{\boldsymbol{\xi}}'\boldsymbol{\xi}']\mathrm{e}^{\mathrm{i}(S_{\mathrm{c}}[\bar{\boldsymbol{\xi}},\,\boldsymbol{\xi}]-S^*_{\mathrm{c}}[\bar{\boldsymbol{\xi}}',\,\boldsymbol{\xi}'])}\mathcal{F}^A_{\alpha i}[\bar{\boldsymbol{\xi}}\boldsymbol{\xi}; \bar{\boldsymbol{\xi}}'\boldsymbol{\xi}']. \tag{14}$$

Similar to the calculation of the influence functional in equation (14), the operator-associated influence functional $\mathcal{F}^A_{\alpha i}[\bar{\boldsymbol{\xi}}\boldsymbol{\xi}; \bar{\boldsymbol{\xi}}'\boldsymbol{\xi}']$ can be evaluated in the same way with the result

$$\mathcal{F}^A_{\alpha i}[\bar{\boldsymbol{\xi}}\boldsymbol{\xi}; \bar{\boldsymbol{\xi}}'\boldsymbol{\xi}'] = -\mathrm{i}\mathcal{A}_{\alpha i}[\boldsymbol{\xi}, \boldsymbol{\xi}']\mathcal{F}[\bar{\boldsymbol{\xi}}\boldsymbol{\xi}; \bar{\boldsymbol{\xi}}'\boldsymbol{\xi}'], \tag{15}$$

where the functional expression of the effective electron annihilation operator is obtained as

$$\mathcal{A}_\alpha[\boldsymbol{\xi}, \boldsymbol{\xi}'] = \int_{t_0}^{t} \mathrm{d}\tau \left\{ \boldsymbol{g}_\alpha(t,\tau)\boldsymbol{\xi}(\tau) - \widetilde{\boldsymbol{g}}_\alpha(t,\tau)\left[\boldsymbol{\xi}(\tau) + \boldsymbol{\xi}'(\tau)\right]\right\}, \tag{16}$$

and $\mathcal{F}[\bar{\boldsymbol{\xi}}\boldsymbol{\xi}; \bar{\boldsymbol{\xi}}'\boldsymbol{\xi}']$ is the same influence functional given by equation (4). It should be pointed out that the factorability of the operator-associated influence functional is due to the fact that the environmental path integral is exactly computable.

Since the path integrals in equation (14) can also be reduced to Gaussian integrals, similar to the derivation of the master equation for the reduced density matrix (8), we use again the stationary phase method to exactly carry out the path integrals of equation (14). The result is

$$\mathcal{J}^A_{\alpha i}(\bar{\boldsymbol{\xi}}_f, \boldsymbol{\xi}'_f, t|\boldsymbol{\xi}_0, \bar{\boldsymbol{\xi}}'_0, t_0) = -\mathrm{i}\mathcal{A}_{\alpha i}(\boldsymbol{\xi}'_f, \boldsymbol{\xi}_0, t)\mathcal{J}(\bar{\boldsymbol{\xi}}_f, \boldsymbol{\xi}'_f, t|\boldsymbol{\xi}_0, \bar{\boldsymbol{\xi}}'_0, t_0), \tag{17}$$

where $\mathcal{A}_{\alpha i}(\boldsymbol{\xi}'_f, \boldsymbol{\xi}_0, t) = \sum_j [\boldsymbol{y}_{\alpha ij}(t)\boldsymbol{\xi}_{0j} + \boldsymbol{z}_{\alpha ij}(t)\boldsymbol{\xi}'_{fj}]$ with $\boldsymbol{y}_\alpha(t) = \int_{t_0}^{t} d\tau\, \boldsymbol{g}_\alpha(t,\tau)\boldsymbol{u}(\tau) + \boldsymbol{z}_\alpha(t)\boldsymbol{u}(t)$ and $\boldsymbol{z}_\alpha(t) = [\boldsymbol{\lambda}_\alpha(t) + \boldsymbol{\kappa}_\alpha(t)\boldsymbol{v}(t)][1 - \boldsymbol{v}(t)]^{-1}$. The propagating function $\mathcal{J}(\bar{\boldsymbol{\xi}}_f, \boldsymbol{\xi}'_f, t|\boldsymbol{\xi}_0, \bar{\boldsymbol{\xi}}'_0, t_0)$ is given by equation (6) in the last section. Substituting equation (17) into (13) and using the identity

$$\boldsymbol{\xi}_0\mathcal{J} = \boldsymbol{u}^{-1}(t)\left\{[1 - \boldsymbol{v}(t)]\frac{\partial}{\partial \boldsymbol{\xi}_f} - \boldsymbol{v}(t)\boldsymbol{\xi}'_f\right\}\mathcal{J},$$

together with the D-algebra for the fermion creation and annihilation operators in the fermion coherent state representation, we obtain the effective electronic annihilation operator after tracing over completely the environmental degrees of freedom,

$$A_{\alpha i}(t) = -\mathrm{i}\sum_j \left\{\boldsymbol{\lambda}_{\alpha ij}(t)[a_j\rho(t) + \rho(t)a_j] + \boldsymbol{\kappa}_{\alpha ij}(t)a_j\rho(t)\right\}, \tag{18}$$

where the coefficient matrices $\boldsymbol{\lambda}_\alpha(t)$ and $\boldsymbol{\kappa}_\alpha(t)$ are the same coefficients given by equation (10) and $\rho(t)$ is just the reduced density matrix determined by master equation (8).

Accordingly, substituting the above result into equation (12), the transient current can be directly calculated, and the result is rather simple,

$$\begin{aligned} I_\alpha(t) &= -\frac{e}{\hbar}\,\mathrm{Tr}\left\{\boldsymbol{\lambda}_\alpha(t) + \boldsymbol{\kappa}_\alpha(t)\boldsymbol{\rho}^{(1)}(t) + \mathrm{H.c.}\right\} \\ &= -\frac{2e}{\hbar}\,\mathrm{Re}\int_{t_0}^{t} d\tau\,\mathrm{Tr}\left\{\boldsymbol{g}_\alpha(t,\tau)\boldsymbol{v}(\tau) - \widetilde{\boldsymbol{g}}_\alpha(t,\tau)\bar{\boldsymbol{u}}(\tau) + \boldsymbol{g}_\alpha(t,\tau)\boldsymbol{u}(\tau)\boldsymbol{u}^{-1}(t)[\boldsymbol{\rho}^{(1)}(t) - \boldsymbol{v}(t)]\right\}, \end{aligned} \tag{19}$$

where the notation Tr is the trace over the states of the central region, $\boldsymbol{\rho}^{(1)}_{ij}(t) \equiv \mathrm{tr}_s[a^\dagger_j a_i \rho(t))]$ is the single-particle density matrix, while the matrix elements of $\boldsymbol{g}_\alpha(\tau, \tau')$ and $\widetilde{\boldsymbol{g}}_\alpha(\tau, \tau')$ are the non-local time correlation functions of the reservoirs given by equation (5), and $\boldsymbol{u}(\tau)$, $\boldsymbol{v}(\tau)$ and $\bar{\boldsymbol{u}}(\tau)$ are determined non-perturbatively by equation (7), as shown in the last section. This is a derivation of the transient current $I_\alpha(t)$ that flows from the lead α into the central region, based on the influence functional.

3.2. The master equation approach

In fact, we can derive the transient current in a rather simple way once we have the exact master equation. Consider the equation of motion for the operator $a_i^\dagger a_j$ in the Heisenberg picture,

$$\mathrm{i}\frac{\mathrm{d}}{\mathrm{d}t}a_i^\dagger a_j = [a_i^\dagger a_j, H] = \sum_l \epsilon_{jl} a_i^\dagger a_l - \epsilon_{li} a_l^\dagger a_j + \sum_{\alpha k}(V_{j\alpha k} a_i^\dagger c_{\alpha k} - V_{i\alpha k}^* c_{\alpha k}^\dagger a_j). \tag{20}$$

Taking the expectation value of the above equation with respect to the state $\rho_{\mathrm{tot}}^{\mathrm{H}}$ (the total density matrix in the Heisenberg picture) and then transforming it into the Schrödinger picture, we obtain

$$\mathrm{i}\frac{\mathrm{d}\boldsymbol{\rho}^{(1)}(t)}{\mathrm{d}t} = [\boldsymbol{\epsilon}(t), \boldsymbol{\rho}^{(1)}(t)] + \mathrm{i}\sum_\alpha \mathcal{I}_\alpha(t). \tag{21}$$

Here, we have used the definition of the single-particle density matrix again, $\boldsymbol{\rho}_{ij}^{(1)}(t) \equiv \mathrm{tr}[a_j^\dagger a_i \rho_{\mathrm{tot}}(t)] = \mathrm{tr}_s[a_j^\dagger a_i \rho(t)]$, and also introduced a current matrix $\mathcal{I}_{\alpha ji}(t) \equiv \mathrm{itr}_s[A_{\alpha i}^\dagger(t) a_j - a_i^\dagger A_{\alpha j}(t)]$. Equivalently, the transient current of equation (12) is simply given by $I_\alpha(t) = \frac{e}{\hbar}\mathrm{Tr}\mathcal{I}_\alpha(t)$. In other words, the equation of motion for $\boldsymbol{\rho}^{(1)}(t)$ is directly related to the transient current.

On the other hand, the equation of motion for the single-particle density matrix can be obtained easily from the exact master equation (8). The result is

$$\begin{aligned}\frac{\mathrm{d}\boldsymbol{\rho}^{(1)}}{\mathrm{d}t} &= \dot{\boldsymbol{u}}\boldsymbol{u}^{-1}\boldsymbol{\rho}^{(1)} + \boldsymbol{\rho}^{(1)}(\boldsymbol{u}^\dagger)^{-1}\dot{\boldsymbol{u}}^\dagger - \widetilde{\boldsymbol{\gamma}} \\ &= -\mathrm{i}[\boldsymbol{\epsilon}, \boldsymbol{\rho}^{(1)}] - (\boldsymbol{\kappa}\boldsymbol{\rho}^{(1)} + \mathrm{H.c.}) - \widetilde{\boldsymbol{\gamma}}.\end{aligned} \tag{22}$$

Using the expression for $\widetilde{\boldsymbol{\gamma}}(t)$ given by (9*c*) and comparing equation (21) with (22), we have

$$\mathcal{I}_\alpha(t) = -\{\boldsymbol{\lambda}_\alpha(t) + \boldsymbol{\kappa}_\alpha(t)\boldsymbol{\rho}^{(1)}(t) + \mathrm{H.c.}\}. \tag{23}$$

The above equation reproduces exactly the transient current of equation (19) after taking a trace over the states of the central system. This not only provides a self-consistent check for the transient current derived from the influence functional but also shows the superiority of the master equation.

Taking the trace over the both sides of equation (21) and also noting that $N(t) = \mathrm{Tr}\boldsymbol{\rho}^{(1)}(t)$, the total electron occupation in the central system, we have

$$e\frac{\mathrm{d}N(t)}{\mathrm{d}t} = \sum_\alpha I_\alpha(t) \equiv -I_{\mathrm{dis}}(t), \tag{24}$$

where $I_{\mathrm{dis}}(t)$ is defined as the transient displacement current [46]. This shows that the sum over the currents flowing from all the leads into the central region equals the change in the electron occupation in the central region, as was expected. In the steady-state limit $t \to \infty$, $\dot{N}(t) = \mathrm{Tr}\dot{\boldsymbol{\rho}}^{(1)}(t) = 0$ so that $I_{\mathrm{dis}}(t) = 0$, as a consequence of current conservation.

3.3. Solution to single-particle density matrix and transient current

To show the power of the master equation, we will further evaluate the single-particle density matrix explicitly from the master equation. To do so, let us rewrite equation (9*c*) as

$$\frac{\mathrm{d}\boldsymbol{v}}{\mathrm{d}t} = \dot{\boldsymbol{u}}\boldsymbol{u}^{-1}\boldsymbol{v} + \boldsymbol{v}(\boldsymbol{u}^\dagger)^{-1}\dot{\boldsymbol{u}}^\dagger - \widetilde{\boldsymbol{\gamma}}.$$

Comparing equation (21) for the single-particle density matrix $\boldsymbol{\rho}^{(1)}(t)$ and the above equation for $\boldsymbol{v}(t)$ shows that the solution of $\boldsymbol{\rho}^{(1)}(t)$ is just $\boldsymbol{v}(t)$, apart from an initial function. Explicitly, equation (21) and the above equation lead to

$$\frac{\mathrm{d}}{\mathrm{d}t}(\boldsymbol{\rho}^{(1)}-\boldsymbol{v})=\dot{\boldsymbol{u}}\boldsymbol{u}^{-1}(\boldsymbol{\rho}^{(1)}-\boldsymbol{v})+(\boldsymbol{\rho}^{(1)}-\boldsymbol{v})(\boldsymbol{u}^{\dagger})^{-1}\dot{\boldsymbol{u}}^{\dagger}.$$

It is easy to find from the above equation the following relationship between $\boldsymbol{\rho}^{(1)}(t)$ and $\boldsymbol{v}(t)$,

$$\boldsymbol{\rho}^{(1)}(t)=\boldsymbol{v}(t)+\boldsymbol{u}(t)\boldsymbol{\rho}^{(1)}(t_0)\boldsymbol{u}^{\dagger}(t), \tag{25}$$

where $\boldsymbol{\rho}^{(1)}(t_0)$ is the initial single-particle density matrix. Accordingly, the transient current (19) is reduced to

$$I_\alpha(t)=-\frac{2e}{\hbar}\,\mathrm{Re}\int_{t_0}^{t}\mathrm{d}\tau\,\mathrm{Tr}\{\boldsymbol{g}_\alpha(t,\tau)\boldsymbol{v}(\tau)-\widetilde{\boldsymbol{g}}_\alpha(t,\tau)\bar{\boldsymbol{u}}(\tau)+\boldsymbol{g}_\alpha(t,\tau)\boldsymbol{u}(\tau)\boldsymbol{\rho}^{(1)}(t_0)\boldsymbol{u}^{\dagger}(t)\}. \tag{26}$$

The last term shows the explicit dependence on the initial state in the transient current, where the initial state is presented through the initial single-particle density matrix $\boldsymbol{\rho}^{(1)}(t_0)$. $\boldsymbol{\rho}^{(1)}(t_0)$ contains information about the initial electron occupation in each level as well as the electron quantum coherence between different levels in the central region. This term is also an important ingredient in the study of transient dynamics for practical manipulation of a quantum device in the real-time domain, namely, *it determines explicitly the time evolution of electrons in nanodevices from some initial preparation towards any specifically designed state within a given time*.

As one can find in appendix B, this explicit initial-state dependence is often omitted in practical applications of Keldysh's non-equilibrium Green function technique (also see [7]). The Green function technique has the advantage of treating the single-particle density matrix in a complicated system by the assumption of adiabatically switching on the many-body correlations. This allows one to trace back the initial time $t_0\to-\infty$, which provides a great simplification for practical evaluation but in the meantime excludes a good treatment of transient phenomena. The influence functional aims to address the dissipative dynamics of an open system in terms of the reduced density matrix (an arbitrary quantum state) [22]. The master equation derived (if possible) from the influence functional explicitly determines, by definition, the temporal evolution of an initially prepared state. For the nanodevices considered in this paper, we are able to obtain a convolutionless form of the exact master equation so that all the non-Markovian memory effects are encoded into the time-dependent coefficients in the master equation. These time-dependent coefficients are determined by the functions $\boldsymbol{u}(t)$ and $\boldsymbol{v}(t)$ (see equation (9)), which are closely related to the retarded and less Green functions in Keldysh's formalism, as we have shown in appendix A. Therefore, all the advantages of the non-equilibrium Green function technique are maintained in our master equation theory. However, the difficulty of addressing the transient dynamics can be avoided in terms of the master equation.

3.4. Relation between the transient current and the reduced density matrix

Furthermore, the transient current defined by equation (12) can be written as a trace over the transient current operator: $I_\alpha(t)=(e/\hbar)\mathrm{tr}_{\mathrm{s}}[\boldsymbol{I}_\alpha(t)]$, where the current operator $\boldsymbol{I}_\alpha(t)$ is obtained directly from equation (18),

$$\boldsymbol{I}_\alpha(t)=-\sum_{ij}\{\boldsymbol{\lambda}_{\alpha ij}(t)[a_i^{\dagger}a_j\rho(t)+a_i^{\dagger}\rho(t)a_j]+\boldsymbol{\kappa}_{\alpha ij}(t)a_i^{\dagger}a_j\rho(t)+\mathrm{H.c.}\}\equiv\mathcal{L}_\alpha^{+}(t)\rho(t). \tag{27}$$

Here, we have introduced a current superoperator $\mathcal{L}_\alpha^+(t)$ such that the current operator can be simply expressed as the current superoperator acting on the reduced density matrix. Note, from equation (10), that $\sum_\alpha(\boldsymbol{\lambda}_\alpha+\boldsymbol{\lambda}_\alpha^\dagger)=\widetilde{\boldsymbol{\gamma}}$ and $\sum_\alpha(\boldsymbol{\kappa}_\alpha+\boldsymbol{\kappa}_\alpha^\dagger)=2\boldsymbol{\gamma}$, and the transient current operator given by equation (27) is closely connected to master equation (8) for the reduced density matrix $\rho(t)$.

Because of the trace over the states of the central system, the transient current of equation (12) can be alternatively expressed as

$$I_\alpha(t)=\mathrm{i}\frac{e}{\hbar}\,\mathrm{tr}_\mathrm{s}\sum_i\left[a_iA_{\alpha i}^\dagger(t)-A_{\alpha i}(t)a_i^\dagger\right]\equiv-\frac{e}{\hbar}\,\mathrm{tr}_\mathrm{s}\widetilde{\boldsymbol{I}}_\alpha(t), \tag{28}$$

where $\widetilde{\boldsymbol{I}}_\alpha(t)$ can be considered as an inverse current operator of electrons with respect to $\boldsymbol{I}_\alpha(t)$. Then, using equation (18) again, we have

$$\widetilde{\boldsymbol{I}}_\alpha(t)=\sum_{ij}\{\boldsymbol{\lambda}_{\alpha ij}(t)[a_j\rho(t)a_i^\dagger+\rho(t)a_ja_i^\dagger]+\boldsymbol{\kappa}_{\alpha ij}(t)a_j\rho(t)a_i^\dagger+\mathrm{H.c.}\}\equiv\mathcal{L}_\alpha^-(t)\rho(t), \tag{29}$$

where $\mathcal{L}_\alpha^-(t)$ is defined as the superoperator for the inverse current operator $\widetilde{\boldsymbol{I}}_\alpha(t)$. Now it is easy to check that master equation (8) for the reduced density matrix and the transient current of (19) can be simply expressed as

$$\begin{cases}\dfrac{\mathrm{d}\rho(t)}{\mathrm{d}t}=-\mathrm{i}[H_\mathrm{S}(t),\rho(t)]+\displaystyle\sum_\alpha[\mathcal{L}_\alpha^+(t)+\mathcal{L}_\alpha^-(t)]\rho(t),\\[2ex] I_\alpha(t)=\dfrac{e}{\hbar}\mathrm{tr}_\mathrm{s}[\mathcal{L}_\alpha^+(t)\rho(t)]=-\dfrac{e}{\hbar}\mathrm{tr}_\mathrm{s}[\mathcal{L}_\alpha^-(t)\rho(t)],\end{cases} \tag{30}$$

where H_S is the original Hamiltonian of the central system. This analytical operator relation between the reduced density matrix and the transient current shows explicitly the intimate connection between quantum decoherence and quantum transport in non-equilibrium dynamics. The reservoir-induced non-Markovian relaxation and decoherence in the transport processes are manifested through the superoperators of (27) and (29) acting on the reduced density matrix $\rho(t)$. The time-dependent parameters $\boldsymbol{\lambda}_\alpha(t)$ and $\boldsymbol{\kappa}_\alpha(t)$ appearing in the superoperators are given by equation (10), which are determined by the integrodifferential equations of motion (7). This completes the non-equilibrium theory for transient electron dynamics in the nanostructures we are concerned with.

We now summarize the main results derived in this section. We obtain the general formula of the transient current $I_\alpha(t)$ through the lead α, which is given by equation (19) or equivalently equation (26), accompanied by the exact master equation for the reduced density matrix $\rho(t)$. We also establish explicitly the connection between the transient current and the reduced density matrix, i.e. equation (30), through the superoperators $\mathcal{L}_\alpha^+(t)$ and $\mathcal{L}_\alpha^-(t)$ determined by equations (27) and (29), which encompass all the back-reaction effects associated with the non-Markovian dynamics of the central system interacting with the lead α. This general non-equilibrium theory for electron transient dynamics is valid for arbitrary bias and gate voltage pulses with arbitrary couplings between the central system and the leads. These results enable us to analyze the transient quantum transport phenomena intimately entangled with the electron quantum coherence and non-Markovian dynamics through the reduced density matrix. The latter describes completely the temporal evolution of electron quantum coherence in the nanodevice. Therefore, the problem we posed in the Introduction, 'the big challenge is to understand and

predict not only how fast or slow the device can turn a current on or off, but also how reliably and efficiently the device can manipulate quantum coherence of the electron states through external bias and gate voltage controls', can now be well addressed within the master equation theory.

4. Analytical and numerical illustrations

4.1. Time-independent bias voltage in the wide band limit (WBL): an analytic solution for transient dynamics

As an illustration, we apply the theory developed in this paper to SETs, or, more specifically, a single dot containing only one spinless level coupled to left and right leads. The Hamiltonian of the central system is simply written as $H = \epsilon a^\dagger a$. This system contains only two states, the empty state $|0\rangle$ and the occupied state $|1\rangle$. All the corresponding matrices (denoted by the bold symbols) in the previous sections are then reduced to a single function, such as $\boldsymbol{u}(t) = u(t)$, $\boldsymbol{v}(t) = v(t)$ and $\boldsymbol{\rho}^{(1)}(t) = \langle 1|\rho|1\rangle = \rho_{11}(t) = N(t)$. We will first consider a time-independent bias voltage V. For simplicity, we also assume that the tunneling couplings between the leads and the dot as well as the densities of states of the leads are energy independent. In other words, the spectral density becomes a constant $\Gamma_\alpha(\omega) = \Gamma_\alpha$. The non-local time correlation functions are reduced to

$$g_\alpha(\tau - \tau') = \Gamma_\alpha \delta(\tau - \tau'), \tag{31a}$$

$$\widetilde{g}_\alpha(\tau - \tau') = \Gamma_\alpha \int \frac{\mathrm{d}\omega}{2\pi} f_\alpha(\omega)\, \mathrm{e}^{-\mathrm{i}\omega(\tau-\tau')}. \tag{31b}$$

This corresponds to the WBL in the literature.

To be explicit, we take the initial time $t_0 = 0$ and let $e = \hbar = 1$ in the following calculations. In the WBL, the solution of equation (7) is

$$u(\tau) = \exp\left\{-\left(\mathrm{i}\epsilon + \frac{\Gamma}{2}\right)\tau\right\}, \quad \bar{u}(\tau) = u^\dagger(t - \tau), \tag{32a}$$

$$v(t) = v_{\mathrm{st}} + \int \frac{\mathrm{d}\omega}{2\pi} \frac{\Gamma_\mathrm{L} f_\mathrm{L}(\omega) + \Gamma_\mathrm{R} f_\mathrm{R}(\omega)}{(\epsilon - \omega)^2 + (\Gamma/2)^2} \left\{\mathrm{e}^{-\Gamma t} - 2\mathrm{e}^{-\Gamma t/2}\cos[(\epsilon - \omega)t]\right\}, \tag{32b}$$

where $\Gamma = \Gamma_\mathrm{L} + \Gamma_\mathrm{R}$ and v_{st} is the solution of $v(t)$ at the steady-state limit,

$$v_{\mathrm{st}} = \int \frac{\mathrm{d}\omega}{2\pi} \frac{\Gamma_\mathrm{L} f_\mathrm{L}(\omega) + \Gamma_\mathrm{R} f_\mathrm{R}(\omega)}{(\epsilon - \omega)^2 + (\Gamma/2)^2} = \rho^{(1)}_{\mathrm{st}}. \tag{33}$$

The electron occupation of the dot is calculated using equation (25) as

$$N(t) = \rho^{(1)}(t) = \mathrm{e}^{-\Gamma t}\rho^{(1)}(0) + v(t), \tag{34}$$

where $N(0) = \rho^{(1)}(0)$ is the initial electron occupation of the dot. Obviously, in the steady-state limit, $N_{\mathrm{st}} = v_{\mathrm{st}}$. This is not surprising since $\rho^{(1)}(t)$ and $v(t)$ obey the same equation of motion that must lead to the same result in the steady-state limit.

The transient current can then be analytically obtained, as follows,

$$I_\alpha(t) = I_{\alpha,\mathrm{st}} - \Gamma_\alpha[N(t) - N_{\mathrm{st}}] - \mathrm{e}^{-\Gamma t/2} \int \frac{\mathrm{d}\omega}{2\pi} \frac{\Gamma_\alpha f_\alpha(\omega)}{(\epsilon - \omega)^2 + (\Gamma/2)^2} \times \{\Gamma\cos[(\epsilon - \omega)t] - 2(\epsilon - \omega)\sin[(\epsilon - \omega)t]\}, \tag{35}$$

where the steady-state current is

$$I_{\alpha,\mathrm{st}} = \Gamma_\alpha \int \frac{\mathrm{d}\omega}{2\pi} \frac{\Gamma_\mathrm{L}[f_\alpha(\omega) - f_\mathrm{L}(\omega)] + \Gamma_\mathrm{R}[f_\alpha(\omega) - f_\mathrm{R}(\omega)]}{(\epsilon-\omega)^2 + (\Gamma/2)^2}. \tag{36}$$

Due to charge conservation, it is necessary to check the displacement current that obeys the relation (24). In the WBL,

$$\begin{aligned} I_\mathrm{dis}(t) &= \Gamma \mathrm{e}^{-\Gamma t} N(0) - \int \frac{\mathrm{d}\omega}{2\pi} \frac{\Gamma_\mathrm{L} f_\mathrm{L}(\omega) + \Gamma_\mathrm{R} f_\mathrm{R}(\omega)}{(\epsilon-\omega)^2 + (\Gamma/2)^2} \\ &\quad \times \left\{ -\Gamma \mathrm{e}^{-\Gamma t} + \Gamma \mathrm{e}^{-\Gamma t/2} \cos[(\epsilon-\omega)t] + 2(\epsilon-\omega)\mathrm{e}^{-\Gamma t/2} \sin[(\epsilon-\omega)t] \right\} \\ &= -\frac{\mathrm{d}N(t)}{\mathrm{d}t}. \end{aligned} \tag{37}$$

At the steady-state limit, the displacement current $I_\mathrm{dis}(t \to \infty) = 0$, as a consequence of current conservation. It is also straightforward to calculate the net current,

$$\begin{aligned} I_\mathrm{net}(t) &= I_\mathrm{L}(t) - I_\mathrm{R}(t) \\ &= I_\mathrm{st} - (\Gamma_\mathrm{L} - \Gamma_\mathrm{R})[N(t) - N_\mathrm{st}] - \mathrm{e}^{-\Gamma t/2} \int \frac{\mathrm{d}\omega}{2\pi} \frac{\Gamma_\mathrm{L} f_\mathrm{L}(\omega) - \Gamma_\mathrm{R} f_\mathrm{R}(\omega)}{(\epsilon-\omega)^2 + (\Gamma/2)^2} \\ &\quad \times \{\Gamma \cos[(\epsilon-\omega)t] - 2(\epsilon-\omega)\sin[(\epsilon-\omega)t]\}, \end{aligned} \tag{38}$$

where the stationary net current is

$$I_\mathrm{st} = 2\Gamma_\mathrm{L}\Gamma_\mathrm{R} \int \frac{\mathrm{d}\omega}{2\pi} \frac{f_\mathrm{L}(\omega) - f_\mathrm{R}(\omega)}{(\epsilon-\omega)^2 + (\Gamma/2)^2}. \tag{39a}$$

As we can see, once we solve the integrodifferential equations of motion, equation (7), a complete time dependence of all the physical quantities, such as the electron occupations in the central system and the currents flowing from each lead to the central region, can be obtained with explicit dependence on the time and the initial electron occupation without ambiguity. From equation (35), we see that the initial current $I_\alpha(0) = -\Gamma_\alpha N(0)$, which depends on the initial occupation of the dot. This result is consistent with the electron occupation in the dot (equation (34)). For zero initial occupation, the initial current is zero. Note that some of the above results were also obtained recently using the non-equilibrium Green function technique [12].

4.2. Non-Markovian memory structure

Realistically, the spectral density of the leads must depend on the energy. Here, we take the energy dependence as a Lorentzian-type form [9, 10, 13],

$$\Gamma_\alpha(\omega) = \frac{\Gamma_\alpha W_\alpha^2}{(\omega - \mu_\alpha)^2 + W_\alpha^2}, \tag{40}$$

where Γ_α describes the coupling strength and W_α is the bandwidth of the source (drain) reservoir with $\alpha = L(R)$. Obviously, the WBL, $\Gamma_\alpha(\omega) = \Gamma_\alpha$, is achieved by simply letting $W_\alpha \to \infty$. The lead correlation functions with time-independent voltage can be parameterized as [10]

$$g_\alpha(t-\tau) = \frac{\Gamma_\alpha W_\alpha}{2} \mathrm{e}^{-\gamma_{\alpha 0}(t-\tau)}, \tag{41a}$$

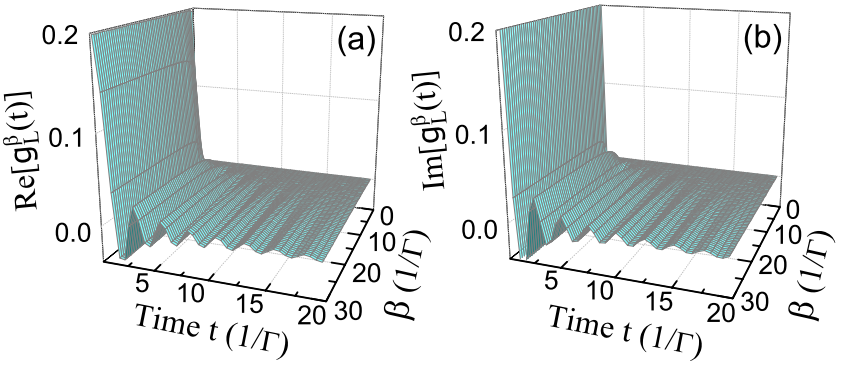

Figure 2. Three-dimensional plot of the temperature-dependent non-local time correlation function $\widetilde{g}_{\rm L}(t-\tau)$ (denoted by $g_{\rm L}^{\beta}(t-\tau)$ in the plots, in unit: Γ^2) as a function of temperature for $\mu_{\rm L}=2.5\Gamma$ and $\Gamma_{\rm L}=0.5\Gamma$. V = 5 (arbitrary units).

$$\widetilde{g}_{\alpha}(t-\tau)=\sum_{m=0}^{M}\eta_{\alpha m}{\rm e}^{-\gamma_{\alpha m}(t-\tau)}. \tag{41b}$$

The first term in equation (41*b*) with $m=0$ arises from the pole of the spectral density function, with

$$\eta_{\alpha 0}=\frac{\Gamma_{\alpha}W_{\alpha}/2}{1+{\rm e}^{-{\rm i}\beta_{\alpha}W_{\alpha}}},\qquad \gamma_{\alpha 0}=W_{\alpha}+{\rm i}\mu_{\alpha}. \tag{42}$$

The other terms with $m>0$ ($M\to\infty$ in principle) arise from the Matsubara poles, where the relevant parameters are explicitly given as

$$\eta_{\alpha m}=\frac{\rm i}{\beta_{\alpha}}\Gamma_{\alpha}(-{\rm i}\gamma_{\alpha m}),\qquad m=1,\ldots,\infty, \tag{43a}$$

$$\gamma_{\alpha m}=\frac{(2m-1)\pi}{\beta_{\alpha}}+{\rm i}\mu_{\alpha}. \tag{43b}$$

In fact, the bandwidth W_{α} in a Lorentizan-type spectral density is the main factor leading to the non-Markovian dynamics in the transient transport. In the WBL, $W_{\alpha}\to\infty$, the dominating memory structure is mostly washed out. This can be seen directly from the reservoir correlation functions. The correlation function $g_{\alpha}(t-\tau)$ of equation (41*a*) can be simplified to $\frac{\Gamma_{\alpha}}{2}\delta(t-\tau)$ in the WBL. For $\widetilde{g}_{\alpha}(t-\tau)$ in equation (41*b*), the first term ($m=0$) is also simplified to a delta function of $t-\tau$ but the other terms ($m\geqslant 1$) are apparently not changed too much,

$$\widetilde{g}_{\alpha}(t-\tau)\to\frac{\Gamma_{\alpha}}{2(1+{\rm e}^{-{\rm i}\beta_{\alpha}W_{\alpha}})}\delta(t-\tau)+\frac{\rm i}{\beta_{\alpha}}\Gamma_{\alpha}\sum_{m=1}^{M}{\rm e}^{-\gamma_{\alpha m}(t-\tau)}. \tag{44}$$

The profile of this temperature-dependent time correlation function is plotted in figure 2. When we take further the high temperature limit $\beta_{\alpha}\to 0$, the summation term in equation (44) will also be reduced to a delta function of $t-\tau$ (see figure 2). Then no memory effect remains, and a true Markov limit is reached at the high temperature limit. On the other hand, in the large bias voltage limit $eV=\mu_{\rm L}-\mu_{\rm R}\to\infty$, we have $f_{\rm L}(\omega+\frac{eV}{2})\to 1$ and $f_{\rm R}(\omega-\frac{eV}{2})\to 0$, which lead

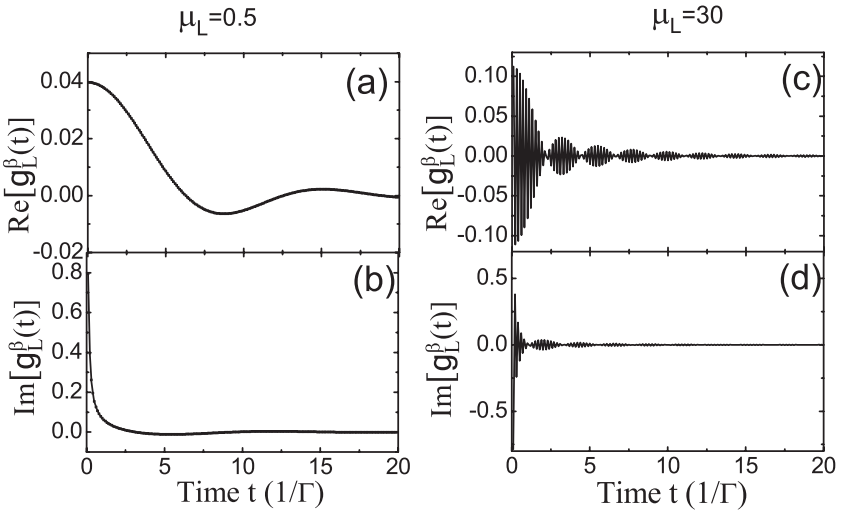

Figure 3. The temperature-dependent non-local time correlation function $\widetilde{g}_{\rm L}(t-\tau)$ with different bias voltages at a fixed temperature $\beta^{-1} = k_{\rm B}T = 0.1\Gamma$ and $\Gamma_{\rm L} = 0.5\Gamma$. (a and b) The plots for $\mu_{\rm L} = 0.5\Gamma$ and (c and d) the plots for $\mu_{\rm L} = 30\Gamma$ (the large bias limit). $\Gamma_{\rm L} = 0.5$, $\beta = 20$ (arbitrary units).

to $\widetilde{g}_{\rm L}(t-\tau) \to g_{\rm L}(t-\tau) = \frac{\Gamma_{\rm L}}{2}\delta(t-\tau)$ and $\widetilde{g}_{\rm R}(t-\tau) \to 0$ in the WBL. This reduces the electron dynamics into the Markov limit again, as has been widely used in the literature [47]–[49]. However, for a relatively low temperature or a finite bias voltage, there appears to exist some non-Markovian effect in the WBL, coming from the summation term in equation (44). Figure 3 shows the time dependence of the correlation dependence for different voltages. As one can see, the temperature-dependent time-correlation function does not approach a delta function of the time.

To examine whether some non-Markovian effect can still survive in the WBL, we numerically calculate the transient current passing through a SET considered in the last subsection. In the sequential tunneling regime $\mu_{\rm L} > \epsilon > \mu_{\rm R}$, the exact solutions of the occupation and the transient current are close to the Markov limit (differing by a few per cent except for a very short timescale at the beginning), as shown in figures 4(a)–(d). In the co-tunneling regime with $\mu_\alpha \gg \epsilon$, the exact solutions of the occupation and the current are still almost the same as their Markov counterparts except for the very short timescale at the beginning (see figures 4(e)–(f)). These results indicate that the WBL (an extremely short characteristic time of the reservoirs) largely suppresses the thermal fluctuations. In other words, when the bandwidth $W \to \infty$, not only at the high temperature and large bias limit, but even for a finite temperature and a finite bias voltage, the non-Markovian effects become quite weak and are most likely negligible. Thus, the WBL mainly takes into account the Markov dynamics. The manifestation of the non-Markovian memory structure then should go beyond the WBL [13]. In figure 5, we calculate the transient current with different bandwidths to demonstrate the non-Markovian effect in transport phenomena. As we can see, the transport dynamics are significantly different from the Markov limit for a small W. Increasing the value of W will decrease the memory effect accordingly. When the bandwidth $W \geqslant 50\Gamma$, the exact solution of the transient current nearly approaches the Markov result that is consistent with the WBL. An analysis of the non-Markovian dynamics in this simple system has also recently been carried out using the Heisenberg equations of motion [50].

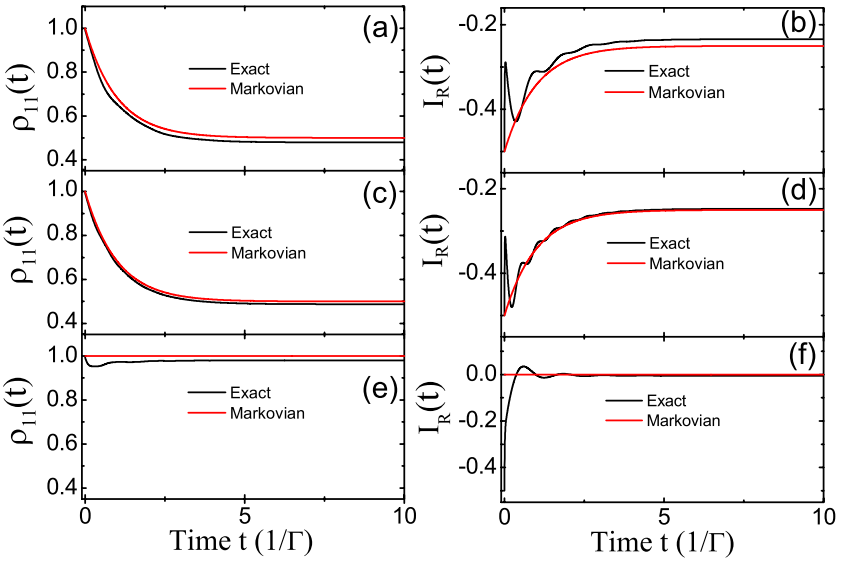

Figure 4. Comparison of the non-Markovian dynamics with the Markov limit in the WBL for the electron occupation (left row) and the transient current (right row). Here, we used the parameters $\Gamma_L = \Gamma_R = 0.5\Gamma$, $\beta^{-1} = k_B T = 0.1\Gamma$, $\mu_{L,R} = \pm eV/2 = \pm 5\Gamma$ and (a and b) $eV = 10\Gamma$, $\epsilon = 2\Gamma$; (c and d) $eV = 20\Gamma$, $\epsilon = 2\Gamma$; (e and f) $eV = 10\Gamma$, $\epsilon = -10\Gamma$. $\rho_{11}(0) = 1.0$; $\mu_L = \mathrm{eV}/2 = -\mu_R$, $\Gamma_L = \Gamma_R = 0.5\Gamma$, $\beta^{-1} = 0.1\Gamma$, $I_R(t)$ unit:$e\hbar/\Gamma$.

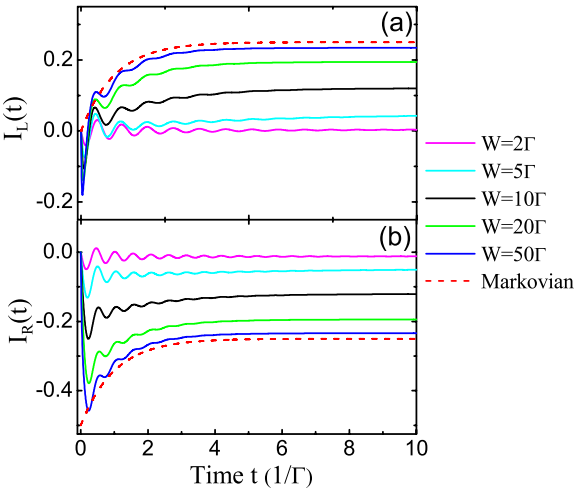

Figure 5. The transient current $I_{L,R}(t)$ through the left and right leads with a Lorentzian-type spectral density for different bandwidths: dashed line, the WBL ($W = \infty$); other lines, from top to bottom for (a) and from bottom to top for (b), correspond to $W = 50$, 20, 10, 5, 2 and Γ, respectively. Other parameters that we used are $\Gamma_L = \Gamma_R = 0.5\Gamma$, $\beta^{-1} = k_B T = 0.1\Gamma$, $\mu_{L,R} = \pm eV/2 = \pm 5\Gamma$ and $\epsilon = 2\Gamma$. $\rho_{11}(0) = 1.0$; $\mu_L = \mathrm{eV}/2 = -\mu_R$, $\Gamma_L = \Gamma_R = 0.5\Gamma$, $\beta^{-1} = 0.1\Gamma$, $\mathrm{eV} = 10\Gamma$, $I(t)$ unit:$e\hbar/\Gamma$.

4.3. Transient transport dynamics with time-dependent bias voltage

We are now in a position to study the time-dependent transport phenomena cooperating with the solution of the master equation in response to time-dependent bias voltages. The calculation of the time-dependent electron current in response to time-dependent bias voltages has recently received much attention [7, 9, 12, 15, 36]. Transient transport dynamics are also a central ingredient of many different experiments, such as single-electron pumps and turnstiles with time-modified gate signals moving electrons one by one through quantum dots [51]–[54], and the study of the quantum capacitance and inductances with ac voltage response [55]–[59]. All these problems can be studied explicitly in the present theory. The corresponding nanoscale devices can be modeled as the SET considered in this section. The applied time-dependent voltages are taken to be the most commonly interesting ones. For the time-dependent voltages, as we mentioned in section 2, the single-particle energy levels of the leads are changed to $\epsilon_{\alpha k}(t) = \epsilon_{\alpha k} + eV_\alpha(t)$. The non-local time correlation functions of the leads can be expressed as

$$g_\alpha(\tau, \tau') = \exp\left\{-ie\int_{\tau'}^{\tau} d\tau_1 V_\alpha(\tau_1)\right\} g_\alpha(\tau - \tau'), \tag{45a}$$

$$\widetilde{g}_\alpha(\tau, \tau') = \exp\left\{-ie\int_{\tau'}^{\tau} d\tau_1 V_\alpha(\tau_1)\right\} \widetilde{g}_\alpha(\tau - \tau'). \tag{45b}$$

With the parametrization of equation (41), it is not difficult to numerically calculate the transient electron dynamics for arbitrary bandwidth W_α. In the following calculation, we use symmetric ac voltages, i.e. $\mu_L(t) = eV(t)/2$ and $\mu_L(t) = -eV(t)/2$. For the quantum dot with a single level, the reduced density matrix can be fully characterized by the electron occupation in the dot. The exact numerical results for the time-dependent occupation and current due to different types of applied ac voltages are presented as follows.

4.3.1. Exponentially time-dependent bias voltage. We shall first study the transient electron dynamics in response to an exponentially time-dependent bias voltage $V(t) = V(1 - e^{-t/\tau})$, where $\tau > 0$ is the time dominating the switch-on rate of the voltage. The asymptotic limit $\tau \to 0^+$ corresponds to a step function. The numerical results are plotted in figure 6. The first peak shown in the displacement current arises from the co-tunneling process during the initially short timescale. At the beginning, the Fermi surface of both the leads is nearly equivalent to zero and the dot energy level is higher than the Fermi surface. The initial currents through both leads are equal to each other due to the totally symmetric structure. This leads to zero initial net current. This feature is common for other types of ac bias voltage discussed later. In general, the emergence of the peaks in the current corresponds to a steep transient behavior of the electron states (i.e. the occupation for the single-level dot) occurring inside the dot. The nonlinear response to time-dependent bias is clearly manifested in the change in both the electron state in the dot and the transient current through the leads (including the individual current through each lead and the displacement and net currents), as is plotted in figure 6. In particular, the net current changes in time closely follow the change in electron occupation in the dot, while the displacement current depicts a steep change in the rate of occupation, as we expected from equation (24).

4.3.2. Oscillating bias voltage. Let us now move to the transient electron dynamics driven by an oscillating voltage [7], $V(t) = V_0 - V_c \cos(\omega_c t)$, where V_0 is a dc component, and V_c and

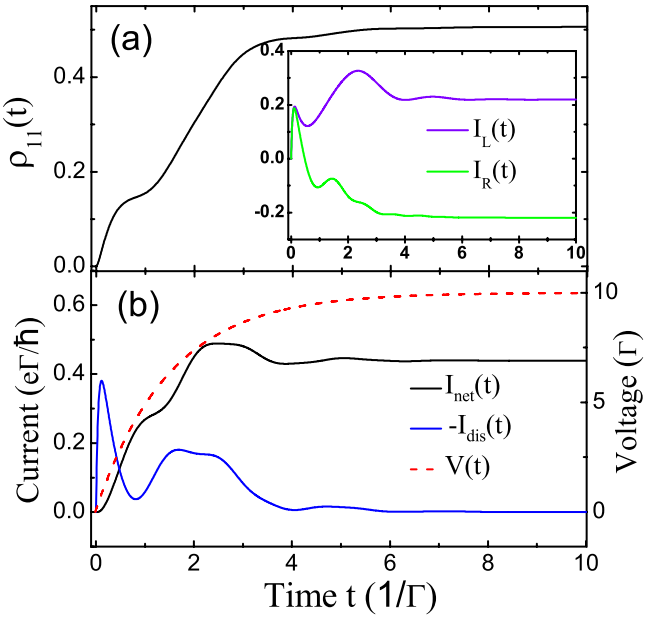

Figure 6. The occupation and transient currents in response to exponential time-dependent voltage with $\tau = 1.5/\Gamma$. The other parameters are $eV = 10\Gamma$, $\Gamma_L = \Gamma_R = 1.5\Gamma$, $\beta^{-1} = k_B T = 0.1\Gamma$, $W_L = W_R = W = 20\Gamma$ and $\epsilon = 2\Gamma$. $\rho_{11}(0) = 0.0$; $\varepsilon = 2.0\Gamma$, $V_c = V_0 = 10.0\Gamma$, $\mu_L = V/2 = -\mu_R$, $\Gamma_L = \Gamma_R = 0.5$, $\beta = 10\Gamma$; $\tau_a = 1.5/\Gamma$ (arbitrary units).

ω_c are the oscillation amplitude and frequency of the ac component. The corresponding exact numerical solution is shown in figure 7. As one can see, all the quantities, the electron state in the dot and the transient currents, have similar oscillating behavior to the ac voltage oscillation, where the steady-state values and the oscillation around the steady-state values are determined by the dc voltage V_0. The oscillation amplitude around the steady state is proportional to the ac voltage amplitude V_c and the oscillation period is mainly given by $T = 2\pi/\omega_c$. However, the transient dynamics of the occupation and current do not always strictly follow the ac voltage oscillation. The current oscillation is a little slantwise compared to the ac voltage oscillation. By increasing the amplitude of the ac voltage V_c and decreasing the oscillation frequency ω_c, a sideband oscillation occurs in the electron occupation as well as in the transient currents, as shown in figure 8. Physically, this sideband oscillation is induced by the sinusoidal behavior of the ac voltage. It can be understood analytically under the WBL [7],

$$\tilde{g}_\alpha(\tau, \tau') = \sum_{n_1,n_2} J_{n_1}\left(\frac{\Delta_\alpha}{\omega_c}\right) J_{n_2}\left(\frac{\Delta_\alpha}{\omega_c}\right) \int \frac{d\omega}{2\pi}\, \Gamma_\alpha f_\alpha(\omega) e^{-i(\omega+n_1\omega_c)\tau} e^{i(\omega+n_2\omega_c)\tau'}, \tag{46a}$$

$$v(t) = \sum_{\alpha,n_1,n_2} J_{n_1}\left(\frac{\Delta_\alpha}{\omega_c}\right) J_{n_2}\left(\frac{\Delta_\alpha}{\omega_c}\right) \int \frac{d\omega}{2\pi}\, \Gamma_\alpha f_\alpha(\omega) \times \frac{e^{-\Gamma t} + e^{-i(n_1-n_2)\omega_c t} - e^{-\Gamma/2 t}\left[e^{-i(\epsilon-\omega-n_2\omega_c)t} + e^{i(\epsilon-\omega-n_1\omega_c)t}\right]}{(\epsilon-\omega-n_1\omega_c)(\epsilon-\omega-n_2\omega_c) + (\frac{\Gamma}{2})^2 - i\frac{\Gamma}{2}(n_1-n_2)\omega_c}, \tag{46b}$$

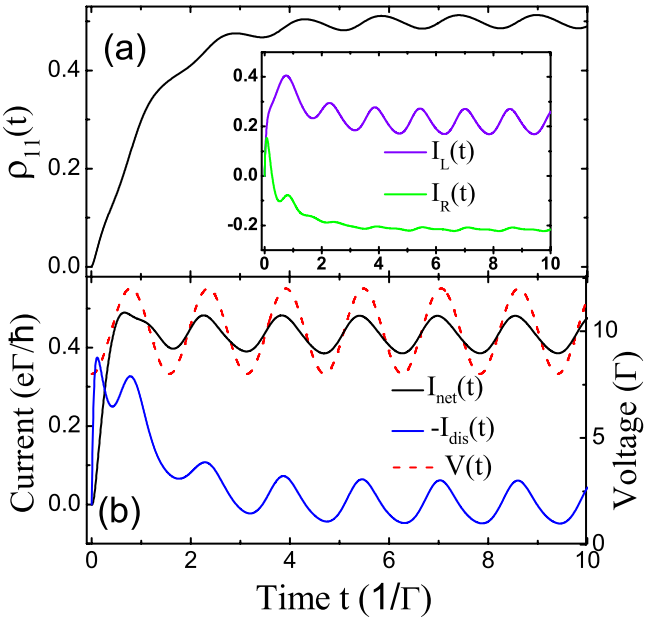

Figure 7. The occupation and transient current in response to oscillating voltage with the dc component $eV_0 = 10\Gamma$, an ac component $eV_c = 2\Gamma$ and the oscillation frequency $\omega_c = 4\Gamma$. The other parameters are the same as in figure 6. $\rho_{11}(0) = 0.0$; $\varepsilon = 2.0$, $\omega = 4$, $\mu_L = V/2 = -\mu_R$, $\Gamma_L = \Gamma_R = 0.5$, $\beta = 10$ (unit: $\Gamma = \Gamma_L + \Gamma_R$) $V_c = 2.0$; $V_0 = 10.0$.

$$I_\alpha(t) = -\Gamma_\alpha \left\{ (\mathrm{e}^{-\Gamma t} N(t_0) + \mathrm{Re}[v(t)] \right\} + \sum_{n_1,n_2} J_{n_1}\left(\frac{\Delta_\alpha}{\omega_c}\right) J_{n_2}\left(\frac{\Delta_\alpha}{\omega_c}\right) \int \frac{\mathrm{d}\omega}{2\pi}\, \Gamma_\alpha f_\alpha(\omega)$$
$$\times\, 2\mathrm{Im} \frac{\mathrm{e}^{-\mathrm{i}(\epsilon-\omega-n_2\omega_c)t} - \mathrm{e}^{-\mathrm{i}(n_1-n_2)\omega_c t}}{\epsilon - \omega - n_2\omega_c + \mathrm{i}\frac{\Gamma}{2}}, \qquad (46c)$$

where the Bessel function satisfies $J_{-n}(z) = (-1)^n J_n(z)$ and $\Delta_{L,R} = \mp\frac{eV_c}{2}$. The numerical result with Lorentzian spectra presented here is qualitatively similar to the previous calculation with the WBL based on the non-equilibrium Green function technique [7].

4.3.3. Gaussian pulse. The last example that we shall study is the transient electron dynamics driven by a Gaussian pulse $V(t) = V \exp\{-\frac{(t-\tau_1)^2}{\tau_2^2}\}$. The width and the center of the pulse are determined by τ_2 and τ_1, respectively. The exact numerical result plotted in figure 9 shows that the net current peak emerges (slightly delayed) just after the voltage pulse, while the corresponding response of the electron occupation is delayed significantly. This behavior is easy to understand because the external voltage pulse leads to a sharp change in the electron occupation due to the delayed response. The shape change of the transient current comes from the largest change rate of the electron occupation in the dot. The delayed response effect is determined by the tunneling rate Γ. Outside the voltage pulse, the tunneling current comes completely from the co-tunneling effect and the occupation in the dot decays to a stationary value. It is interesting to note that the response of the occupation and the currents to the

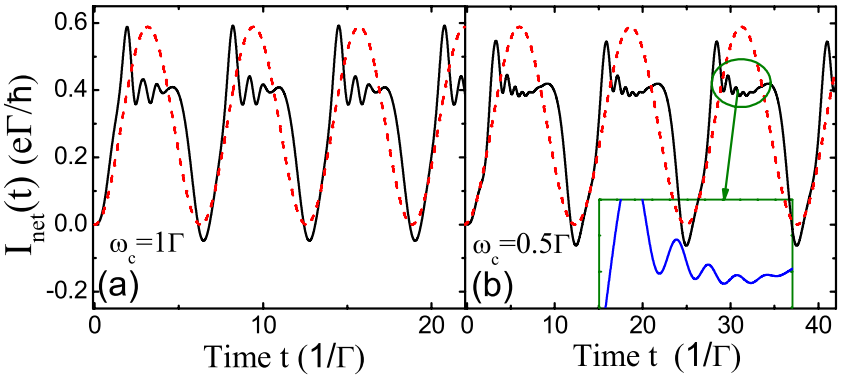

Figure 8. The transient current (black line) in response to the oscillating voltage (dashed red line) with $eV_0 = eV_c = 10\Gamma$ and the oscillating frequencies $\omega_c = 1\Gamma$ for (a) and $\omega_c = 0.5\Gamma$ for (b). The other parameters are the same as in figure 7. $\rho_{11}(0) = 0.0$; $\varepsilon = 2.0$, $\mu_L = V/2 = -\mu_R$, $\Gamma_L = \Gamma_R = 0.5$, $\beta = 10$; $V = V_c = 10.0$.

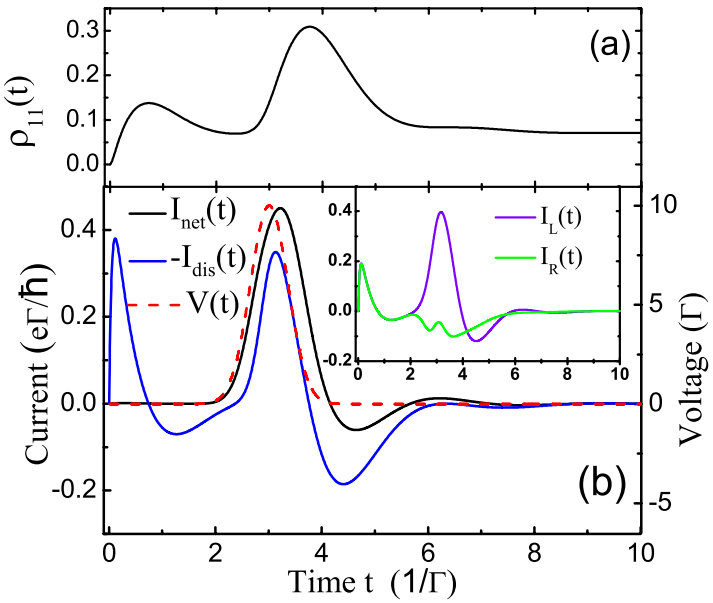

Figure 9. The occupation and transient current in response to Gaussian voltage pulse with $\tau_1 = 3/\Gamma$ and $\tau_2 = 0.5/\Gamma$. The other parameters are the same as in figure 6. $\rho_{11}(0) = 0.0$; $\varepsilon = 2\Gamma$, $V_c = V_0 = 10.0\Gamma$, $\mu_L = V/2 = -\mu_R$, $\Gamma_L = \Gamma_R = 0.5$, $\beta = 10\Gamma$ (arbitrary units) $\tau_1 = 3/\Gamma$, $\tau_2 = 1.5/\Gamma$.

co-tunneling process is different before and after the voltage pulse. Before the voltage pulse, the system is dominated by the co-tunneling process because the Fermi surface of both leads is nearly equivalent but is lower than the dot energy level ($\mu_L \simeq \mu_R \simeq 0 < \epsilon = 2\Gamma$). The aligned Fermi surfaces double the peak amplitude of the displacement current, which also gives the zero net current, while the occupation has a corresponding change with respect to the change of the displacement current. With increasing voltage, the Fermi surface of the left lead moves up over the dot energy level, while that of the right lead moves down

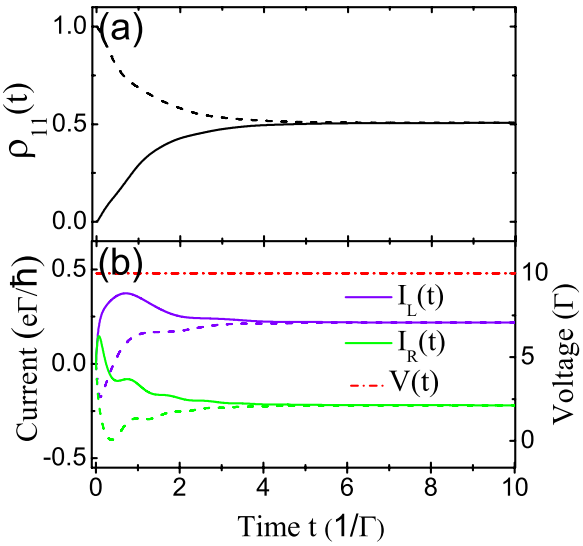

Figure 10. The occupation and transient current in response to a step pulse voltage (i.e. a constant bias after $t = 0$, dot-dashed line) corresponds to the initial condition of $\rho_{11}(t_0) = 0$ (solid lines) and $\rho_{11}(t_0) = 1.0$ (dashed lines), respectively. The other parameters are the same as in figure 6. $\rho_{11}(0) = 0.0$; $\varepsilon = 2.0\Gamma$, $V_c = V_0 = 10.0\Gamma$, $\mu_L = V/2 = -\mu_R$, $\Gamma_L = \Gamma_R = 0.5$, $\beta = 10\Gamma$; $\tau_a = 1.5/\Gamma$ (unit: Γ).

below the dot energy level, such that the system gradually approaches the sequential tunneling regime. This drives the electron flowing from the left lead to the dot and then to the right lead. Such a process results in a sensitive response of all physical quantities, the electron occupation in the dot, the displacement and the net currents. Then, with the voltage decaying to zero, the electron residing in the dot favors co-tunneling into the left lead, which gives a negative current and finally reaches the steady state. The transient electron dynamics with the nonlinear response to this Gaussian pulse are, in particular, interesting for quantum feedback control of the electron states in the dot through the transient current that we will study in the future.

Note that the above transient dynamics start with a zero initial occupation, i.e. $\rho_{00}(t_0) = 1$ and $\rho_{11}(t_0) = 1 - \rho_{00}(t_0) = 0$ [$N(t_0) = 0$]. This implies that the last term of equation (26), which is often ignored in the non-equilibrium Green function technique [9, 27], has no contribution to the transient current in the above numerical calculations. When the dot is initially occupied, the time-dependent current will be quite different, although the steady-state limit is the same, because the initial electron distribution vanishes in the steady-state limit for this simple system. In figure 10, we show the exact numerical result corresponding to such a situation where we take the simple step-pulse voltage as an example. This shows that the initial occupation in the central region has measurable contributions to studying the transient dynamics, especially for the ultrafast (extremely short time) operations in a quantum device.

Combining all these analyses together, as one can see, the exact numerical solutions presented here have demonstrated that both the electron states in the dot and the transient currents passing through it have a clear nonlinear response to the external bias voltage pulses, in particular within a short timescale after the pulse is turned on. These ultrafast nonlinear

response properties should provide very useful information regarding the manipulation of the device states as well as the quantum feedback controls for practical applications. However, since we consider here only a very simple device (a SET with a single-level dot), the quantum coherence and decoherence dynamics in the transient current are not manifested in these numerical calculations. To demonstrate the quantum coherence properties in the transient transport dynamics, it is necessary to have a device containing at least two levels (or a single level with electron spin degrees of freedom) in the central region. Also, in the above numerical calculations, we take a rather large finite bandwidth, $W_\alpha = 20\Gamma$. The non-Markovian memory structure will become more significant when the bandwidth becomes narrower [9, 13]. We will examine in detail these features within the present theory in our future work.

5. Summary and perspective

In summary, we have established a non-equilibrium quantum theory for the transient electron dynamics of various nanodevices, based on the Feynman–Vernon influence functional. We have extended the exact master equation, equation (8), obtained recently [13], to nanodevices in which all constituents of the device vary in time in response to time-dependent external fields. The master equation takes a convolutionless form and hence the non-Markovian dynamics are fully encoded in the time-dependent coefficients. Explicitly, the back-reaction effect of the gating electrodes on the central system is fully taken into account by these time-dependent coefficients through the integrodifferential equations of motion (7). The non-Markovian memory structure is non-perturbatively built into the integral kernels in these equations of motion. All the physical observables can be calculated directly from the master equation. In particular, the transient transport current, equation (19) or (26), and the single particle density matrix, equation (25), are found directly from the master equation in a rather simple way, where the initial state dependence of the transport current shows up explicitly (see equation (26)). The master equation and the transient transport current are also explicitly related to each other in terms of the superoperators acting on the reduced density matrix (see equation (30)). This exact non-equilibrium formalism should provide a very intuitive picture showing how the change in the electron quantum coherence in the devices is intimately related to the electron tunneling processes through the leads and therefore responds nonlinearly to the corresponding external bias controls. This theory is applicable to a variety of quantum decoherence and quantum transport phenomena involving the non-Markovian memory effect, in both stationary and transient scenarios, and at arbitrary initial temperatures of the different contacts.

As we have also shown in the appendices, we can simply reproduce the non-equilibrium transport theory in terms of the non-equilibrium Green function technique. However, we should point out that the quantum transport theory based on the non-equilibrium Green function technique does not explicitly give the connection to the reduced density matrix of the device and thereby lacks a direct description of the quantum decoherence processes of the electrons and the non-Markovian memory dynamics in nanostructures. However, the way in which the quantum decoherence and the non-Markovian memory affect the electron transport is the central issue in the investigation of the non-equilibrium quantum transport. Our theory builds on the master equation of the reduced density matrix. The non-equilibrium transport current is directly derived from the reduced density matrix. The master equation for the reduced density matrix (i.e. equation (8), which provides all the information about the electron quantum coherence in the device) plus the transient current (i.e. equation (26), which determines transient

electron transport phenomena, including the initial state dependence) together provide a unique procedure to address the quantum decoherence problem in nonequilibrium quantum transport.

As a simple illustration, we apply the theory to a SET, a simple model of electron tunneling through a single-level quantum dot. We obtain all analytical solutions in the WBL where the dependence of the initial electron occupation in the dot is explicitly determined. Taking a more realistic spectral density with a Lorentzian shape, we show that the Markov limit is a good approximation in the WBL. The non-Markovian memory effect is dominated by a finite bandwidth of the spectral density. Under ac bias voltage pulses (including a step pulse, a Gaussian pulse and an oscillation pulse), we have demonstrated the ultrafast nonlinear response of the electron occupation and currents to the ac bias. We find that the transient currents are more sensitive to the energetic configuration of the dot than the temporal evolution of the electron occupation. More applications will be presented in future work. These include the decoherence transport dynamics in quantum dot devices, such as quantum dot Aharonov–Bohm inteferometers; the non-equilibrium dynamics and the real-time monitoring of spin polarization processes in nanostructures; the transient transport dynamics in molecular electronics; and the application to bio-electronics, such as DNA junctions, etc.

Lastly, we should also point out that the present theory is developed without considering the electron–electron interaction in the device and therefore it is mainly valid in the weak Coulomb interaction regime. It is not difficult to extend the present theory to the strong Coulomb blockage regime by properly excluding the doubly occupied states in the central region of the nanostructure, as we have shown explicitly in [13]. Although studying the above two extreme limits, the extremely weak and the extremely strong Coulomb interaction regimes, together could lead to a significant understanding of quantum devices in practical applications, there is an increasing amount of discussion about the intermediate Coulomb interaction regime [60, 61], where the analysis of transport physics becomes much more complicated. We should simply outline the possible extension of the present theory to the intermediate Coulomb interaction regime. In this situation, the path integrals of equations (3) and (14) may not be carried out exactly, and therefore it is not obvious that one can find an analytically closed formulation for the exact master equation of the reduced density matrix and an exact expression of the time-dependent transport current. But the master equation, equation (8), and the transient transport current, equation (26), can still serve as a good approximation with respect to the saddle point approximation [26] or more systematically the loop expansion [25], where the Coulomb interaction can be included self-consistently in generalizing integrodifferential equations of motion (7). Such a generalization should provide a systematic procedure for the study of quantum transport phenomena in the intermediate Coulomb interaction regime. The detailed extension of the present theory to the interacting electron systems is now in progress and will be published separately.

Acknowledgment

We thank Ora Entin-Wohlman for useful discussions and for helping us to improve the presentation of the manuscript. This work was supported by the National Science Council (NSC) of ROC under contract no. NSC-96-2112-M-006-011-MY3, the National Natural Science Foundation of China under grant no. 10904029 and the Research Grants Council of Hong Kong (604709). We are also grateful to the National Center for Theoretical Science of the NSC for support.

Appendix A. Relations between $\boldsymbol{u}(t)$, $\bar{\boldsymbol{u}}(\tau)$, $\boldsymbol{v}(t)$ and the non-equilibrium Green functions

As we see, both the master equation (8) and the transient current (26) are completely determined by the propagating matrices of the stationary paths: $\boldsymbol{u}(\tau)$, $\bar{\boldsymbol{u}}(\tau)$ and $\boldsymbol{v}(\tau)$. Here, we shall show that these propagating matrices are directly related to the retarded, advanced and lesser Green functions in the non-equilibrium Green function technique. In our previous work [13], the propagating matrices $\boldsymbol{u}(\tau)$, $\bar{\boldsymbol{u}}(\tau)$ and $\boldsymbol{v}(\tau)$ were introduced to simplify the stationary path equations of motion (with the convention $\boldsymbol{x} = \boldsymbol{y}\boldsymbol{z}$ for $x_i = \sum_j y_{ij} z_j$), as follows,

$$\boldsymbol{\xi}(\tau) = \boldsymbol{u}(\tau)\boldsymbol{\xi}(t_0) + \boldsymbol{v}(\tau)[\boldsymbol{\xi}(t) + \boldsymbol{\xi}'(t)], \tag{A.1a}$$

$$\boldsymbol{\xi}(\tau) + \boldsymbol{\xi}'(\tau) = \bar{\boldsymbol{u}}(\tau)[\boldsymbol{\xi}(t) + \boldsymbol{\xi}'(t)]. \tag{A.1b}$$

In fact, equations (A.1) show that $\boldsymbol{u}(\tau)$ is a propagating matrix of the forward stationary paths $\boldsymbol{\xi}(\tau)$ starting at t_0, while $\boldsymbol{v}(\tau)$ mixes the forward path $\boldsymbol{\xi}(\tau)$ and the backward path $\boldsymbol{\xi}'(\tau)$ started backwardly from t, and $\bar{\boldsymbol{u}}(\tau)$ is a backward-propagating matrix of the stationary paths. In fact, equations (A.1) show that the transformation matrices $\boldsymbol{u}(\tau)$, $\bar{\boldsymbol{u}}(\tau)$ and $\boldsymbol{v}(\tau)$ should be defined more precisely as $\boldsymbol{u}(\tau) \equiv \mathsf{u}(\tau, t_0)$, $\bar{\boldsymbol{u}}(\tau) \equiv \mathsf{u}^\dagger(t, \tau)$ and $\boldsymbol{v}(\tau) \equiv \mathsf{v}(\tau, t)$:

$$\boldsymbol{\xi}(\tau) = \mathsf{u}(\tau, t_0)\boldsymbol{\xi}(t_0) + \mathsf{v}(\tau, t)[\boldsymbol{\xi}(t) + \boldsymbol{\xi}'(t)], \tag{A.2a}$$

$$\boldsymbol{\xi}(\tau) + \boldsymbol{\xi}'(\tau) = \mathsf{u}^\dagger(t, \tau)[\boldsymbol{\xi}(t) + \boldsymbol{\xi}'(t)], \tag{A.2b}$$

where the Grassmannian variables $\boldsymbol{\xi}(\tau)$ and $\boldsymbol{\xi}'(\tau)$ represent the forward and backward electron paths in the functional path integrals. Then equations (A.1) directly tell us that $\mathsf{u}(\tau, t_0)$ describes the electron propagation (represented by $\boldsymbol{\xi}(\tau)$ in the Grassmannian space) from the initial time t_0 to the time τ so that it is just the retarded Green function, namely,

$$\begin{aligned} \boldsymbol{u}(\tau) &= \mathsf{u}(\tau, t_0) = \mathrm{i}\boldsymbol{G}^r(\tau, t_0) \\ &= \theta(\tau - t_0)\langle\{a_i(\tau), a_j^\dagger(t_0)\}\rangle. \end{aligned} \tag{A.3}$$

Similarly, $\mathsf{u}^\dagger(t, \tau)$ describes the inverse propagation of the electron (or the backward propagation represented by $\boldsymbol{\xi}'(\tau)$) from time t to time τ such that it is indeed the advanced Green function,

$$\bar{\boldsymbol{u}}(\tau) = \mathsf{u}^\dagger(t, \tau) = -\mathrm{i}\boldsymbol{G}^a(\tau, t). \tag{A.4}$$

In the meantime, in the same way, equation (7*a*) indicates that the time correlation function of the α-reservoir,

$$\begin{aligned} \boldsymbol{g}_{\alpha ij}(\tau_1, \tau_2) &= \mathrm{i}\boldsymbol{\Sigma}^r_{\alpha ij}(\tau_1, \tau_2) \\ &= \theta(\tau_1 - \tau_2) \sum_k V_{\alpha ki} V^*_{\alpha kj} \langle\{c_{\alpha k}(\tau_1), c^\dagger_{\alpha k}(\tau_2)\}\rangle_{\mathrm{B}}, \end{aligned} \tag{A.5}$$

as a back-reaction effect of the α-lead to the central system, is the retarded self-energy. These relations can be justified by equations (7*a*) and (7*b*).

The function $\mathsf{v}(\tau, t)$ describes the electron propagation mixing the forward and backward paths so that it is related to the lesser Green function defined by $\boldsymbol{G}^<_{ij}(\tau, t) \equiv \mathrm{i}\langle a_j^\dagger(t) a_i(\tau)\rangle$ in the

non-equilibrium Green function formalism. In fact, it is not difficult to find the explicit solution of equation (7*c*),

$$\boldsymbol{v}(\tau) = \mathrm{v}(\tau, t) = \int_{t_0}^{\tau} \mathrm{d}\tau_1 \int_{t_0}^{t} \mathrm{d}\tau_2\, \mathrm{u}(\tau, \tau_1)\widetilde{\boldsymbol{g}}(\tau_1, \tau_2)\mathrm{u}^{\dagger}(t, \tau_2), \tag{A.6}$$

which in terms of Green functions becomes

$$\mathrm{v}(\tau, t) = -\mathrm{i}\int_{t_0}^{\tau} \mathrm{d}\tau_1 \int_{t_0}^{t} \mathrm{d}\tau_2\, \boldsymbol{G}^{r}(\tau, \tau_1)\boldsymbol{\Sigma}^{<}(\tau_1, \tau_2)\boldsymbol{G}^{a}(\tau_2, t), \tag{A.7}$$

where

$$\boldsymbol{\Sigma}^{<}(\tau_1, \tau_2) = \mathrm{i}\widetilde{\boldsymbol{g}}(\tau_1, \tau_2) \tag{A.8}$$

is the lesser component of the self-energy. On the other hand, the single-particle reduced density matrix is related to the lesser Green function by $\boldsymbol{\rho}^{(1)}(t) = -\mathrm{i}\boldsymbol{G}^{<}(\tau, t)|_{\tau=t}$. From the relation of equation (25), we find that $\boldsymbol{v}(\tau)$ is related to the lesser Green function, as follows,

$$\begin{aligned}\boldsymbol{G}^{<}(\tau, t) &= \mathrm{i}[\boldsymbol{u}(\tau)\boldsymbol{\rho}^{(1)}(t_0)\boldsymbol{u}^{\dagger}(t) + \boldsymbol{v}(\tau)] \\ &= \boldsymbol{G}^{r}(\tau, t_0)\boldsymbol{G}^{<}(t_0, t_0)\boldsymbol{G}^{a}(t_0, t) \\ &\quad + \int_{t_0}^{\tau} \mathrm{d}\tau_1 \int_{t_0}^{t} \mathrm{d}\tau_2\, \boldsymbol{G}^{r}(\tau, \tau_1)\boldsymbol{\Sigma}^{<}(\tau_1, \tau_2)\boldsymbol{G}^{a}(\tau_2, t).\end{aligned} \tag{A.9}$$

This provides indeed the general solution of the lesser Green function with an explicit dependence on the initial states, which has not been solved in the non-equilibrium Green function technique. In the previous investigation of transient electron dynamics, this initial state-dependent term (the first term in equation (A.9)) is often omitted [7, 9, 27]. In fact, the second term in equation (A.9) can only be identified as the lesser Green function $\boldsymbol{G}^{<}(\tau, t)$ in the steady-state limit.

Appendix B. Reproduce the transient current and its steady-state limit in Keldysh's formalism

Using the above explicit relations between $\boldsymbol{u}(t)$, $\bar{\boldsymbol{u}}(\tau)$, $\boldsymbol{v}(t)$ and the non-equilibrium retarded, advanced and lesser Green functions, we immediately obtain the time-dependent current of equation (26) in terms of the non-equilibrium Green functions,

$$I_{\alpha}(t) = -\frac{2e}{\hbar}\mathrm{Re}\int_{t_0}^{t} \mathrm{d}\tau\, \mathrm{Tr}\{\boldsymbol{\Sigma}_{\alpha}^{r}(t, \tau)\boldsymbol{G}^{<}(\tau, t) + \boldsymbol{\Sigma}_{\alpha}^{<}(t, \tau)\boldsymbol{G}^{a}(\tau, t)\}. \tag{B.1}$$

This current has the same form as obtained from the non-equilibrium Green function technique [7, 27]. However, as we have pointed out in practical applications, one usually uses the steady-state lesser Green function, namely ignores the first term in equation (A.9). This term does vanish in the steady-state limit in the simple systems, as we considered in section 4, so that it does not affect the steady-state current. It can also be dropped if one takes the initial time $t_0 \to -\infty$ so that the central region is assumed to be in an empty state initially. However, this term that explicitly depends on the initial single-particle density matrix of the central region (including the initial electron occupation in each level and the electron quantum coherence between different levels in the central region) is crucial for practical manipulation of a real quantum device. Only in the WBL where the non-local time correlation function

$$\boldsymbol{g}_{\alpha}(t, \tau) = \mathrm{i}\boldsymbol{\Sigma}_{\alpha}^{r}(t, \tau) = \boldsymbol{\Gamma}_{\alpha}\delta(t - \tau), \tag{B.2}$$

the integral of the first term in equation (B.1) is reduced to the single-particle density matrix, $\boldsymbol{G}^<(t,t) = i\boldsymbol{\rho}^{(1)}(t)$), which results in

$$I_\alpha(t) = -\frac{e}{\hbar}\mathrm{Tr}\left[\boldsymbol{\Gamma}_\alpha\boldsymbol{\rho}^{(1)}(t) - \boldsymbol{\Gamma}_\alpha\int\frac{\mathrm{d}\omega}{\pi}f_\alpha(\omega) \times\int_{t_0}^{t}\mathrm{d}\tau\,\mathrm{Im}\left\{\mathrm{e}^{-\mathrm{i}[\omega(t-\tau)+e\int_\tau^t \mathrm{d}\tau' V_\alpha(\tau')]}\boldsymbol{G}^a(\tau,t)\right\}\right]. \tag{B.3}$$

Thus, the ignored initial occupation dependence is accidentally recovered in the WBL. In this case, the initial state dependence may not be essential.

To reproduce the steady-state current in terms of the non-equilibrium Green functions and the Landauer–Büttiker formula used in the literature, we introduce the spectral density of the lead α: $\boldsymbol{\Gamma}_{\alpha ij}(\omega) = 2\pi\sum_k V_{\alpha ik}V^*_{\alpha jk}\delta(\omega-\epsilon_{\alpha k})$ and take a time-independent bias voltage explicitly. Then the two-time correlation functions of the α-lead can be written as

$$\boldsymbol{g}_\alpha(\tau-\tau') = \int\frac{\mathrm{d}\omega}{2\pi}\boldsymbol{\Gamma}_\alpha(\omega)\mathrm{e}^{-\mathrm{i}\omega(\tau-\tau')}, \tag{B.4a}$$

$$\widetilde{\boldsymbol{g}}_\alpha(\tau-\tau') = \int\frac{\mathrm{d}\omega}{2\pi}f_\alpha(\omega)\boldsymbol{\Gamma}_\alpha(\omega)\mathrm{e}^{-\mathrm{i}\omega(\tau-\tau')}, \tag{B.4b}$$

where $f_\alpha(\omega) = 1/(\mathrm{e}^{\beta_\alpha(\omega-\mu_\alpha)}+1)$ is the Fermi distribution function of the α-lead at the initial time t_0. Using the Laplace transformation, i.e. $f(z) = \int_{t_0}^{\infty}\mathrm{d}t\,\mathrm{e}^{-z(t-t_0)}f(t)$ with $z = -\mathrm{i}\omega$, we have

$$\boldsymbol{g}_\alpha(\omega) = \int\frac{\mathrm{d}\omega'}{2\pi}\boldsymbol{\Gamma}_\alpha(\omega')\frac{\mathrm{i}}{\omega-\omega'+i0^+} = \mathrm{i}\boldsymbol{\Sigma}^r_\alpha(\omega), \tag{B.5}$$

i.e. $\boldsymbol{g}_\alpha(\omega)$ is the retarded self-energy in the frequency domain. The Laplace transformation of equation (7*a*) for $\boldsymbol{u}(t)$ gives

$$\boldsymbol{u}(\omega) = \frac{\mathrm{i}}{\omega-\boldsymbol{\epsilon}-\boldsymbol{\Sigma}^r(\omega)} = \mathrm{i}\boldsymbol{G}^r(\omega), \tag{B.6}$$

where $\boldsymbol{G}^r(\omega)$ is just the retarded Green function in the frequency domain, and $\boldsymbol{\Sigma}^r(\omega)$ sums over $\boldsymbol{\Sigma}^r_\alpha(\omega)$ for all α. The advanced Green function is simply given by $\bar{\boldsymbol{u}}(\omega) = -\mathrm{i}\boldsymbol{G}^a(\omega) = \boldsymbol{u}^\dagger(\omega)$. Furthermore, for the time-independent Hamiltonian, the explicit solution of equation (7*c*) is

$$\boldsymbol{v}(\tau) = \int_{t_0}^{\tau}\mathrm{d}\tau_1\int_{t_0}^{t}\mathrm{d}\tau_2\,\boldsymbol{u}(\tau_1)\widetilde{\boldsymbol{g}}(\tau-\tau_1-t+\tau_2)\boldsymbol{u}^\dagger(\tau_2). \tag{B.7}$$

Taking the limits $t_0\to-\infty$ and $t\to\infty$, its Laplace transformation (it becomes indeed a Fourier transformation with the above time limit of $-\infty$ to $+\infty$) gives

$$\begin{aligned}\boldsymbol{v}(\omega) &= \boldsymbol{u}(\omega)\widetilde{\boldsymbol{g}}(\omega)\boldsymbol{u}^\dagger(\omega)\\ &= -\mathrm{i}\boldsymbol{G}^r(\omega)\boldsymbol{\Sigma}^<(\omega)\boldsymbol{G}^a(\omega) = -\mathrm{i}\boldsymbol{G}^<(\omega).\end{aligned} \tag{B.8}$$

Here, we have also used the relation $\widetilde{\boldsymbol{g}}(\omega) = -\mathrm{i}\boldsymbol{\Sigma}^<(\omega)$.

Substituting the above results into equation (26) in the steady-state limit $t\to\infty$ (also plus $t_0\to-\infty$), we obtain the steady-state single-particle reduced density matrix and current,

$$\boldsymbol{\rho}^{(1)}_{\mathrm{st}} = \int\frac{\mathrm{d}\omega}{2\pi}\boldsymbol{G}^r(\omega)\left[\sum_\alpha\boldsymbol{\Gamma}_\alpha(\omega)f_\alpha(\omega)\right]\boldsymbol{G}^a(\omega), \tag{B.9a}$$

$$I_{\alpha,\mathrm{st}} = \frac{ie}{\hbar}\int \frac{\mathrm{d}\omega}{2\pi}\,\mathrm{Tr}\left(\boldsymbol{\Gamma}_\alpha(\omega)\left[\boldsymbol{G}^<(\omega) + f_\alpha(\omega)\{\boldsymbol{G}^r(\omega) - \boldsymbol{G}^a(\omega)\}\right]\right). \tag{B.9b}$$

This reproduces the steady-state current in terms of the non-equilibrium Green functions in the frequency domain that has been widely used. When we consider specifically a system coupled with left (source) and right (drain) electrodes, i.e. $\alpha = \mathrm{L}$ and R, respectively, and also assume that the spectral densities for the left and right leads have the same energy dependence, $\boldsymbol{\Gamma}_\mathrm{L}(\omega) = \lambda\boldsymbol{\Gamma}_\mathrm{R}(\omega)$, where λ is a constant, then the net steady-state current flowing from the left to the right lead is given by

$$\begin{aligned} I_\mathrm{st} &= \frac{2e}{\hbar}\int \frac{\mathrm{d}\omega}{2\pi}\left[f_\mathrm{L}(\omega) - f_\mathrm{R}(\omega)\right]\mathcal{T}(\omega), \\ \mathcal{T}(\omega) &= \mathrm{Tr}\left\{\frac{\boldsymbol{\Gamma}_\mathrm{L}(\omega)\boldsymbol{\Gamma}_\mathrm{R}(\omega)}{\boldsymbol{\Gamma}_\mathrm{L}(\omega)+\boldsymbol{\Gamma}_\mathrm{R}(\omega)}\mathrm{Im}[\boldsymbol{G}^a(\omega)]\right\}. \end{aligned} \tag{B.10}$$

This is the generalized Landauer–Büttiker formula [7].

References

[1] Lu W, Ji Z, Pfeiffer L, West K W and Rimberg A J 2003 *Nature* **423** 422
[2] Hayashi T, Fujisawa T, Cheong H D, Jeong Y H and Hirayama Y 2003 *Phys. Rev. Lett.* **91** 226804
[3] Petta J R, Johnson A C, Taylor J M, Laird E A, Yacoby A, Lukin M D, Marcus C M, Hanson M P and Gossard A C 2005 *Science* **309** 1280
[4] Fujisawa T, Hayashi T and Sasaki S 2006 *Rep. Prog. Phys.* **69** 759
[5] Hanson R, Kouwenhoven L P, Petta J R, Tarucha S and Vandersypen L M K 2007 *Rev. Mod. Phys.* **79** 1217
[6] Datta S 1995 *Electronic Transport in Mesoscopic Systems* (Cambridge: Cambridge University Press)
[7] Haug H and Jauho A P 1998 *Quantum Kinetics in Transport and Optics of Semiconductors (Springer Series in Solid-State Sciences* vol 123*)* (Berlin: Springer)
[8] Imry Y 2002 *Introduction to Mesoscopic Physics* 2nd edn (Oxford: Oxford University Press)
[9] Maciejko J, Wang J and Guo H 2006 *Phys. Rev.* B **74** 085324
[10] Jin J S, Zheng X and Yan Y J 2008 *J. Chem. Phys.* **128** 234703
[11] Mühlbacher L and Rabani E 2008 *Phys. Rev. Lett.* **100** 176403
[12] Schmidt T L, Werner P, Muhlbacher L and Komnik A 2008 *Phys. Rev.* B **78** 235110
[13] Tu M W Y and Zhang W M 2008 *Phys. Rev.* B **78** 235311
Tu M W Y, Lee M T and Zhang W M 2009 *Quantum Inf. Process* **8** 631
[14] Zedler P, Schaller G, Kiesslich G, Emary C and Brandes T 2009 *Phys. Rev.* B **80** 045309
[15] Zheng X, Jin J S, Welack S, Luo M and Yan Y J 2009 *J. Chem. Phys.* **130** 164708
[16] Huang K 1987 *Statistical Mechanics* 2nd edn (New York: Wiley)
[17] Cercignani C 1975 *Theory and Application of the Boltzmann Equation* (Edinburgh: Scottish Academic Press)
[18] Smith H and Jensen H H 1989 *Transport Phenomena* (Oxford: Clarendon)
[19] Breuer H-P and Petruccione F 2002 *The Theory of Open Quantum Systems* (Oxford: Oxford University Press)
[20] Schwinger J 1961 *J. Math. Phys.* **2** 407
Keldysh L V 1965 *Sov. Phys.—JETP* **20** 1018
[21] Kadanoff L P and Baym G 1962 *Quantum Statistical Mechanics* (New York: Benjamin)
[22] Feynman R P and Vernon F L 1963 *Ann. Phys.* **24** 118
[23] Chou K C, Su Z B, Hao B L and Yu L 1985 *Phys. Rep.* **118** 1
[24] Rammer J and Smith H 1986 *Rev. Mod. Phys.* **58** 323
[25] Zhang W M and Wilets L 1992 *Phys. Rev.* C **45** 1900
[26] Kamenev A and Andreev A 1999 *Phys. Rev.* B **60** 2218

[27] Wingreen N S, Jauho A-P and Meir Y 1993 *Phys. Rev.* B **48** 8487
Jauho A-P, Wingreen N S and Meir Y 1994 *Phys. Rev.* B **50** 5528
[28] Leggett A J, Chakravarty S, Dorsey A T, Fisher M P A, Garg A and Zwerger W 1987 *Rev. Mod. Phys.* **59** 1
[29] Zurek W H 1991 *Phys. Today* **44** 36
Zurek W H 2003 *Rev. Mod. Phys.* **75** 715
[30] Caldeira A O and Leggett A J 1983 *Physica* A **121** 587
[31] Haake F and Reibold R 1985 *Phys. Rev.* A **32** 2462
[32] Hu B L, Paz J P and Zhang Y H 1992 *Phys. Rev.* D **45** 2843
[33] Weiss U 2008 *Quantum Dissipative Systems* 3rd edn (Singapore: World Scientific)
[34] Calzetta E and Hu B L 2008 *Nonequilibrium Quantum Field Theory* (New York: Cambridge University Press)
[35] Schoeller H and Schön G 1994 *Phys. Rev.* B **50** 18436
[36] König J, Schmid J, Schoeller H and Schön G 1996 *Phys. Rev.* B **54** 16820
[37] Lee M T and Zhang W M 2008 *J. Chem. Phys.* **129** 224106
[38] Pedersen J N and Wacker A 2005 *Phys. Rev.* B **72** 195330
[39] Welack S, Schreiber M and Kleinekathöfer U 2006 *J. Chem. Phys.* **124** 044712
[40] Harbola U, Esposito M and Mukamel S 2006 *Phys. Rev.* B **74** 235309
[41] Zheng X, Jin J S and Yan Y J 2008 *New J. Phys.* **10** 093016
[42] Ng T K and Lee P A 1988 *Phys. Rev. Lett.* **61** 1768
Glazman L I and Raikh M E 1988 *JETP Lett.* **47** 452
[43] Faddeev L D 1980 *Gauge Fields* (New York: Benjamin-Cummings)
[44] Zhang W M, Feng D H and Gilmore R 1990 *Rev. Mod. Phys.* **62** 867
[45] Feynman R P and Hibbs A R 1965 *Quantum Mechanics and Path Integrals* (New York: McGraw-Hill)
[46] Fransson J, Eriksson O and Sandalov I 2002 *Phys. Rev.* B **66** 195319
[47] Gurvitz S A 1997 *Phys. Rev.* B **56** 15215
Gurvitz S A and Prager Y S 1996 *Phys. Rev.* B **53** 15932
[48] Mozyrsky D, Fedichkin L, Gurvitz S A and Berman G P 2002 *Phys. Rev.* B **66** 161313
[49] Flindt C, Novotny T and Jauho A-P 2004 *Phys. Rev.* B **70** 205334
Novotny T, Donarini A, Flindt C and Jauho A-P 2004 *Phys. Rev. Lett.* **92** 248302
[50] Schaller G, Zedler P and Brandes T 2009 *Phys. Rev.* A **79** 032110
[51] Fujiwara A, Zimmerman N M, Ono Y and Takahashi Y 2004 *Appl. Phys. Lett.* **84** 1323
Fujiwara A, Nishiguchi K and Ono Y 2008 *Appl. Phys. Lett.* **92** 042102
[52] Kirk W P and Reed M A (ed) 1992 *Nanostructures and Mesoscopic Systems* (San Diego, CA: Academic)
[53] Switkes M, Marcus C M, Campman K and Gossard A C 1999 *Science* **283** 1905
[54] Blumenthal M D, Kaestner B, Li L, Giblin S, Janssen T J B M, Pepper M, Anderson D, Jones G and Ritchie D A 2007 *Nat. Phys.* **3** 343
[55] Zheng X, Jin J S and Yan Y J 2008 *J. Chem. Phys.* **129** 184112
[56] Nigg S E, López R and Büttiker M 2006 *Phys. Rev. Lett.* **97** 206804
[57] Wang J, Wang B and Guo H 2007 *Phys. Rev.* B **75** 155336
[58] Zheng X, Wang F, Yam C Y, Mo Y and Chen G H 2007 *Phys. Rev.* B **75** 195127
[59] Mo Y, Zheng X, Chen G H and Yan Y J 2009 *J. Phys.: Condens. Matter* **21** 355301
[60] Chang Y C and Kuo D M-T 2008 *Phys. Rev.* B **77** 245412
[61] Schultz M G and von Oppen F 2009 *Phys. Rev.* B **80** 033302